Journal of Atmospheric and Terrestrial Physics, Vol. 41, pp. 797–839
© Pergamon Press Ltd. 1979. Printed in Northern Ireland

0021-9169/79/0701-0797$02.00/0

Chemistry of the thermosphere and ionosphere

D. G. Torr and M. R. Torr

Space Physics Research Laboratory, University of Michigan, Ann Arbor, Michigan 48109, U.S.A.

National Institute for Telecommunications Research of the South African C.S.I.R., P.O. Box 3718, Johannesburg, South Africa

(*Received* 29 *May* 1978)

Abstract—The ionosphere offers an excellent laboratory for the study of atomic and molecular processes. Densities are low, permitting highly reactive species to accumulate in measurable quantities. Temporal and spatial scales are large, and the solar energy source causes substantial departures from thermodynamic equilibrium. This laboratory has been exploited by the Atmosphere Explorer Program of NASA. Simultaneous measurements of a large number of interrelated atmospheric parameters to altitudes as low as 150 km have provided data that can be analyzed in a quantitative manner to derive precise rates, as functions of temperature, for many important chemical reactions, including the reactions of electronically or vibrationally excited metastable species. Analysis of AE results has provided new information on the photochemical role of N in the thermosphere; the rate coefficients for dissociative recombination of NO^+, O_2^+ and N_2^+; reactions of O^+ with N_2, N_2^+ with O, and O^{2+} with O; and reactions of metastable ions, atoms, and molecules. The progress in our understanding of ionospheric chemistry during the last few years shows the power of space science measurement programs carefully designed to provide rigorous tests of quantitative theoretical predictions.

1. INTRODUCTION

The response of the atmosphere to solar radiation is complex. Figure 1 which depicts Roble's (1975) model of the thermosphere, illustrates the complexity of the interactions involved. Many of these have been explored or extensively surveyed, but it was only with the advent of multi-parameter and multi-satellite measurement programs coupled with incoherent scatter radar measurements of aeronomic parameters and comprehensive laboratory studies of reaction rates that a detailed understanding of the mechanisms involved began to emerge. Results obtained from these studies over the past few years have impacted our understanding of nearly every major process which occurs in the thermosphere. In many cases new processes have been discovered, or old concepts have been discarded or significantly revised. The main reason for recent progress is a marked improvement in the quality of measurements made in aeronomy. On the Atmosphere Explorer satellites for example (cf. Dalgarno *et al.*, 1973), many aeronomic parameters are measured simultaneously with accuracies better than 10%. With this kind of data it has become possible to realize a long standing ambition of aeronomers to use the atmosphere as a laboratory. This review has been limited to results obtained from the Atmosphere Explorer program, which has constituted NASA's main thrust in thermospheric aeronomy during the 1970s.

Figure 2 illustrates schematically the main processes which govern the balance of ionization in the thermosphere. Significant advances have been made during the last 5 years in quantitatively understanding the processes involved. We review the most significant of these below. Emphasis is placed on the identification of new processes, the determination of rate coefficients, and on the role played by metastable species in the chemistry of the ionosphere and thermosphere. We begin this discussion with recent developments in our knowledge of processes which produce ionization in the thermosphere.

2. SOURCES OF IONIZATION

2.1 *Photoionization*

The primary source of ionization in the thermosphere is photoionization of neutral atmospheric constituents by solar extreme ultraviolet radiation. An accurate knowledge of the solar EUV flux as a function of wavelength as well as the related absorption and ionization cross sections is needed to

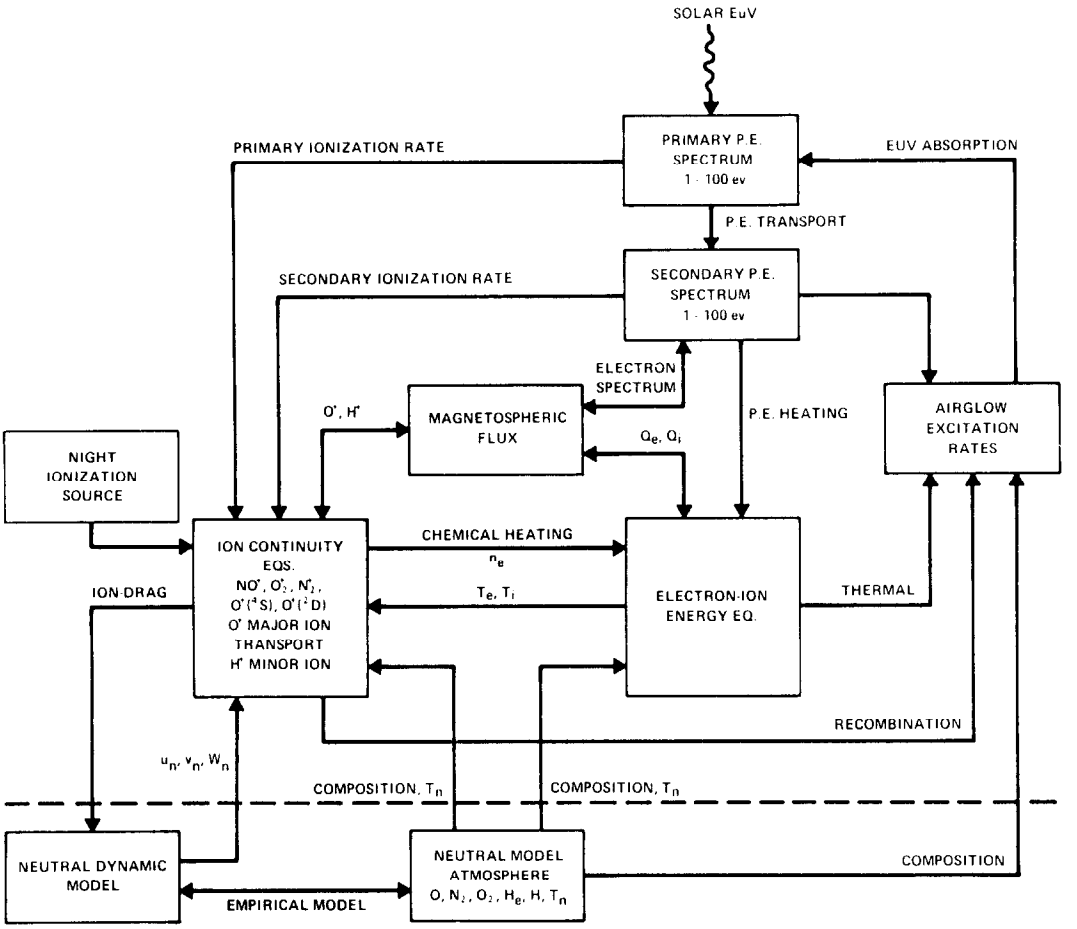

Fig. 1. Block diagram from ROBLE (1975) illustrating the various physical processes which influence the behavior of the ionosphere.

quantitatively model the ionosphere. The most comprehensive measurements of the solar EUV flux made to date are those of HINTEREGGER (1976). These measurements were made by the extreme ultraviolet spectrophotometers on the AE satellites (HINTEREGGER *et al.*, 1973). Measurements have been made since December 1973. Tables of solar flux data have subsequently been published (HINTEREGGER, 1976; HEROUX and HINTEREGGER, 1978; HINTEREGGER *et al.*, 1977) in the form of a summary reference spectrum. The complete reference spectrum tabulated at ~1 Å intervals comprises part of the on-line AE data base. Also available are factors for scaling selected wavelength ranges to reproduce the actual flux for any given day of the year for which measurements are available. These have been published for 1974 (HINTEREGGER *et al.*, 1977).

It has become common practice for many years to scale the solar EUV flux according to variations in the solar 10.7 cm flux. Recent AE EUVS measurements indicate that this procedure is not justified. HINTEREGGER (1978a, b) has observed that the correlation between the EUV and 10.7 cm fluxes is deteriorating with the new solar cycle. The question arises as to whether the degradation in the correlation coefficient will affect neutral densities derived from atmospheric models which use the 10.7 cm flux as a solar index parameter. A comparison of measurements made by the AE open source neutral mass spectrometer (NIER *et al.*, 1973) with atomic oxygen densities derived from the MSIS model atmosphere of HEDIN *et al.* (1974, 1977a, b) indicates a disagreement which has increased over the last 2 years, i.e. 1976–77. [O] appears to be as low as 60% of the MSIS value at 300 km on some orbits.

The relative amplitude of the solar cycle variation in the EUV flux was about one fifth that of the 10.7 cm flux for solar cycle 20 (HINTEREGGER,

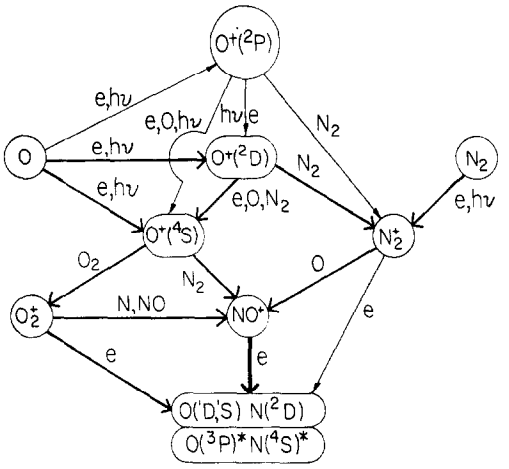

Fig. 2. Schematic illustration of the main processes which govern the balance of ionization in the thermosphere.

1978a). In the new cycle the EUV flux is higher than would be predicted using the 10.7 cm flux while optical depth measurements indicate that the increase in temperature, T_n, is smaller. HINTEREGGER (1978a) suggests that other sources of heat input must exist which are indirectly related to the 10.7 cm solar flux, since the latter currently provides a better index for modeling the neutral atmosphere than the direct measurements of the solar EUV flux. The 10.7 cm flux, however, should be used with caution in scaling tabulated reference values of the EUV flux, and in deriving neutral densities from atmospheric models until more data are available for cycle 21.

Table 1a is a condensed version of HINTEREGGER's preliminary on-line AE R74113 EUV reference spectrum which we have compiled in conjunction with ORSINI (1977). [The R74113 reference spectrum may be obtained from the National Space Science Data Center, Goddard Space Flight Center, Greenbelt, MD, U.S.A. In Table 1b we present a recent update to F74113 published by HINTEREGGER (1978a).] Also included in Table 1a are absorption and ionization cross sections averaged over the same wavelength intervals. The original cross sections comprise part of the AE data base, and are tabulated at the same wavelength intervals as the EUV fluxes given in HINTEREGGER's reference spectrum. The AE cross sections (which were compiled from many sources) will be published by KIRBY-DOCKEN *et al.* (1979).

We have compared production rates obtained with HINTEREGGER's (1976) EUV fluxes and the cross sections of KIRBY-DOCKEN *et al.* (1978) with values derived using the data given in Table 1. The agreement was excellent at altitudes above 150 km. At altitudes below 150 km the attenuated fluxes differed by as much as 30% at large solar zenith angles.

2.2 *Photoelectron impact ionization*

The degradation of the primary photoelectrons ejected in the ionization of neutral constituents is a process of fundamental importance affecting the energetics of the thermosphere. Photoelectrons are a major source of heat and excitation, but only constitute about 25% of the total source of ionization.

The photoelectron flux has been calculated theoretically by numerous workers, and it has been measured experimentally. The most comprehensive set of measurements to date has been made with the AE photoelectron spectrometer (DOERING *et al.*, 1973; PETERSEN *et al.*, 1977). Theoretical results disagree with the AE data by a factor of 2 to 3. Initial calculations by VICTOR *et al.* (1976) were in agreement with measurements made by the AE-C satellite. However, with the launch of AE-E in 1975 the AE-C measurements were subsequently revised and the conflict has not yet been resolved.

Experimenters and theoreticians agree on the shape of the energy spectrum, but disagree on the absolute magnitude by a factor of 2 to 3. The results of VICTOR *et al.* (1976) are in harmony with the more recent and complete calculations of JASPERSE (1978) and PRATHER *et al.* (1978). Recently, NAGY *et al.* (1977) derived results in harmony with the AE data. However, certain problems with one of the input parameters used has been identified which, if corrected, should bring the values of NAGY *et al.* into agreement with the other cited theoretical results. However, this will not resolve all the differences between NAGY *et al.* and the other theoreticians. Currently, the theoretical results of VICTOR *et al.* (1976) are in harmony with other measured geophysical quantities. For example, if the experimental values are correct, theoretical volume emission rates of several emissions would have to be increased significantly. These include the 7320 Å $O^+(^2D–^2P)$ emission (RUSCH *et al.*, 1977a), the *F*-region 5577 Å $O(^1S)$ green line (FREDERICK *et al.*, 1976; KOPP *et al.*, 1977a), the 3371 Å N_2 second positive emission (KOPP *et al.*, 1977b). The theoretical fluxes of VICTOR *et al.* (1976) produce good agreement with the AE measurements of these emissions. An increase in the theoretical photoelectron flux of a factor of 2 to 3 would also detrimentally affect the heat balance studies of HOEGY and BRACE (1978).

Table 1a. Solar flux and cross sections

Designation	λ, Å	$\Phi/10^9$ ph. $cm^{-2}\,s^{-1}$	Total cross section $\sigma_{eff}\times10^{18}$ cm^2 O†	O_2	N_2	Ionization cross sections $\sigma_{eff}\times10^{18}$ cm^2 O†	O_2	N_2
1. H Ly-α	1025.7	2.65	0.00	1.60	0.00	0.00	1.00	0.00
2. C II	1010.2	0.11	0.00	1.40	0.00	0.00	1.30	0.00
3. N III	991.5	0.59	0.00	1.90	1.40	0.00	1.60	0.00
4. Excl. 1, 2, 3	1027–990	0.50	0.00	2.80	0.23	0.00	1.30	0.00
5. C III	977.0	4.40	0.00	21.80	68.10	0.00	1.90	0.00
6. H Ly-γ	972.5	0.60	0.00	21.90	68.10	0.00	1.90	0.00
7. Excl. 5, 6	990–950	0.26	0.00	23.10	45.00	0.00	1.90	0.00
8. H Ly-δ	949.7	0.30	0.00	30.10	7.16	0.00	2.30	0.00
9. S VI	944.5	0.13	0.00	23.40	39.80	0.00	2.40	0.00
10. H Ly-ε	937.8	0.16	0.00	3.20	3.15	0.00	2.60	0.00
11. S VI	933.4	0.14	0.00	25.62	3.13	0.00	2.70	0.00
12. H Ly-Z	930.7	0.26	0.00	3.54	3.13	0.00	2.75	0.00
13. Excl. 8–12	950–912	0.12	0.00	18.20	35.74	0.00	2.70	0.00
14. H Ly-con't.	912–890	4.40	2.96	12.50	46.00	2.96	3.40	0.00
15. H Ly-con't.	890–860	3.80	3.00	10.30	44.30	3.00	3.20	0.00
16. H Ly-con't.	860–840	1.10	3.04	15.10	19.50	3.04	4.30	0.00
17. O II, III	832–835	0.63	3.07	24.00	0.00	3.07	6.50	0.00
18. Excl. 17	840–810	0.86	3.10	28.70	13.70	3.10	7.70	0.00
19.	810–796	0.23	3.10	40.70	21.30	3.10	9.50	0.00
20. OIV	790.21	0.37	3.11	31.20	29.20	3.11	9.60	17.70
21. O IV	787.70	0.20	3.11	30.40	16.26	3.11	9.50	9.85
22. S V	786.50	0.10	3.11	30.20	16.26	3.11	9.60	9.84
23. Ne VIII	780.30	0.22	3.12	28.60	24.70	3.12	10.00	15.14
24. Excl. 20–23	796–780	0.18	3.11	31.10	37.10	3.11	9.60	19.70
25. Ne VIII	770.40	0.28	3.12	24.90	9.72	3.12	9.60	6.60
26. N III, IV	764.60	0.16	3.13	22.70	35.50	3.13	8.50	23.40
27. O V	760.40	0.09	3.13	23.70	30.27	3.13	8.37	19.36
28. Excl. 25–27	780–760	0.17	3.12	24.40	26.20	3.12	9.20	18.20
29.	760–740	0.12	3.13	23.20	27.60	3.13	9.90	18.40
30.	740–732	0.02	3.13	31.60	29.60	3.13	19.00	25.20
31. O III	703.40	0.07	7.23	31.80	26.34	7.23	18.00	20.80
32. Excl. 31	732–700	0.08	7.10	32.90	33.60	7.10	18.60	25.30
33. N III	685.70	0.07	7.36	26.25	26.25	7.36	18.43	21.62
34.	700–665	0.07	7.35	26.20	31.20	7.35	22.30	25.60
35.	665–630	0.04	9.90	25.30	25.00	9.90	21.00	20.70
36. O V	629.73	1.73	10.06	25.85	23.20	10.06	25.85	18.80
37. Mg X	625.28	0.24	10.05	25.82	23.20	10.05	25.82	18.78
38. Mg X	609.85	0.53	10.16	26.13	23.10	10.16	26.13	18.64
39. Excl. 36–37	630–600	0.02	10.11	25.86	23.18	10.11	25.86	18.70
40. O III	599.60	0.16	10.20	26.62	23.11	10.20	26.62	23.11
41. He I	584.33	1.27	10.24	22.01	23.11	10.24	22.01	23.11
42. O IV	554.51	0.72	10.24	25.56	24.74	10.24	25.56	24.74
43. He I	537.03	0.14	10.20	25.20	25.30	10.20	25.20	25.30
44. O III	507.90	0.16	10.06	22.68	22.40	10.06	22.68	22.40
45. SI XII	499.27	0.10	10.00	22.05	21.98	10.00	22.05	21.98
46. Excl. 39–44	600–480	0.47	10.04	22.73	22.64	10.04	22.73	22.64
47. Nc VII	465.22	0.27	9.71	20.39	21.84	9.71	20.39	21.84
48. Excl. 46	480–460	0.08	9.76	20.60	21.70	9.76	20.60	21.70
49.	460–435	0.08	9.52	20.00	22.00	9.52	20.00	22.00
50.	435–400	0.18	9.90	19.40	21.70	9.90	19.40	21.70
51. Mg IX	368.07	0.65	9.26	18.35	17.95	9.26	18.35	17.95
52. Fe XVI	360.76	0.32	9.15	18.12	17.36	9.15	18.12	17.36
53. He II Ly-α	303.78	7.70	8.40	16.00	11.61	8.40	16.00	11.61
54. Excl. 50–52	400–300	0.41	8.72	17.38	15.00	8.72	17.38	15.00
55. Fe XV	284.15	0.21	8.03	14.80	10.58	8.03	14.30	10.58
56. Excl. 54	300–280	0.36	8.22	15.22	10.80	8.22	15.22	10.80
57. Fe XIV	274.24	0.30	7.81	14.09	10.28	7.81	14.09	10.28
58. Fe XIV	264.80	0.24	7.59	13.44	10.01	7.59	13.44	10.01
59. Excl. 56–57	280–260	0.57	7.77	13.95	10.11	7.77	13.95	10.11
60. He II Ly-β, SI χ	256.37	0.52	7.38	12.82	9.65	7.38	12.82	9.65

Table 1a (continued)

Designation	λ, Å	$\Phi/10^9$ ph. cm^{-2} s^{-1}	Total cross section $\sigma_{eff}\times10^{18}$ cm^2 O†	O_2	N_2	Ionization cross sections $\sigma_{eff}\times10^{18}$ cm^2 O†	O_2	N_2
61. Excl. 59	260–240	1.27	7.28	12.40	9.48	7.28	12.40	9.48
62.	240–220	0.52	6.42	10.70	8.35	6.42	10.70	8.35
63.	220–205	0.29	6.14	9.30	7.20	6.14	9.30	7.20
64.	205–190	0.85	5.71	8.35	6.30	5.71	8.35	6.30
65.	190–180	1.00	5.29	7.50	5.60	5.29	7.50	5.60
66.	180–165	1.30	4.96	6.75	5.00	4.96	6.75	5.00
67.	165–138	0.27	4.30	5.32	3.80	4.30	5.32	3.80
68.	138–103	0.08	2.00	4.00	0.90	2.00	4.00	0.90
69.	103–83	0.19	0.70	1.40	0.55	0.70	1.40	0.55
70.	83–62	0.17	0.40	0.80	0.37	0.40	0.80	0.37
71.	62–41	0.11	0.22	0.44	0.18	0.22	0.44	0.18
72.	41–31	5.1(−3)*	0.10	0.20	0.07	0.10	0.20	0.07
73.	31–22.8	1.0(−2)	0.045	0.09	1.00	0.045	0.09	1.00
74.	22.8–15	6.4(−3)	0.35	0.70	0.36	0.35	0.70	0.36
75.	15–10	5.0(−5)	0.135	0.27	0.15	0.135	0.27	0.15
76.	10–5	1.5(−4)	0.037	0.075	0.045	0.037	0.075	0.045
77.	5–3	2.0(−6)	0.006	0.012	0.0065	0.006	0.012	0.0065
78.	3–1	1.0(−3)	0.001	0.002	0.0015	0.001	0.002	0.0015

* $(-3)=\times10^{-3}$

† For: $1\text{ Å}\le\lambda\le665\text{ Å}$
$\sigma(^4S)=0.30\times\sigma(\text{total})$
$\sigma(^2D)=0.45\times\sigma(\text{total})$
$\sigma(^2P)=0.25\times\sigma(\text{total})$

For: $665\text{ Å}<\lambda\le732\text{ Å}$
$\sigma(^4S)=0.43\times\sigma(\text{total})$
$\sigma(^2D)=0.57\times\sigma(\text{total})$
$\sigma(^2P)=0.0$

For: $732\text{ Å}<\lambda\le910\text{ Å}$
$\sigma(^4S)=\sigma(\text{total})$
$\sigma(^2D)=\sigma(^2P)=0.0$

The branching ratios for the ^4S, ^2D and ^2P were calculated by HENRY (1970) (See Table 2 for updated branching ratios).

Table 1b. Comparison of revised reference spectrum F74113, with the preliminary R74113

Wavelength range Å	Photon fluxes 10^9 ph. cm^{-2} s^{-1} F74113	R74113	Ratio *F/R*	Energy fluxes 10^{-3} erg cm^{-2} s^{-1} F74113	R74113	Ratio *F/R*	Number of entries *F*	*R*
50–150	0.55	0.61	0.91	129	141	0.92	185	185
150–250	3.93	4.73	0.83	398	486	0.82	93	95
250–350	11.0	10.8	1.02	736	732	1.01	47	47
350–450	1.35	1.38	0.98	70	73	0.96	56	55
450–550	0.99	1.14	0.87	40	46	0.87	63	66
550–650	4.67	4.55	1.03	155	151	1.03	54	56
650–750	0.62	0.37	1.68	18	10	1.68	105	110
750–850	3.45	3.99	0.87	85	98	0.87	113	112
850–950	6.57	9.55	0.69	145	212	0.69	109	108
950–1050	13.9	13.1	1.06	275	259	1.06	110	108
1050–1150	3.75	4.95	0.76	68	89	0.76	105	106
1150–1250	264	283	0.93	4312	4622	0.93	105	105
1250–1350	16.5	19.7	0.84	250	298	0.84	109	108
1350–1450	17.8	18.7	0.95	252	264	0.95	104	103
1450–1550	45.4	52.6	0.86	599	688	0.87	104	103
1550–1650	95.5	104	0.91	1182	1295	0.91	108	104
1650–1750	355	363	0.98	4135	4221	0.98	105	106
1750–1850	961	924	1.04	10,564	10,164	1.04	103	103
1850–1950	1862	1872	0.99	19,411	19,516	0.99	100	100

From HEROUX and HINTEREGGER (1978).

Note: The intensities given in the wavelength bands include like intensities. This must be taken into account when scaling intensities.

Table 1c. Solar UV reference spectrum F74113 for 23 April 1974

Wavelength, Å	Ion	Intensity incident on Earth 10^9 ph. cm^{-2} s^{-1}	10^{-3} erg cm^{-2} s^{-1}
50–100		0.42	113
100–150		0.15	24
150–200		2.4	271
200–250		1.6	139
256.3	He II, Si X	0.46	36
284.15	Fe XV	0.21	15
250–300		2.3	166
303.78	He II	6.9	450
300–350		8.7	530
368.07	Mg IX	0.65	35
350–400		1.02	55
400–450		0.39	18
465.22	NE VII	0.29	12.4
450–500		0.59	24
500–550		0.49	19
554.37§	O IV	0.72	26
584.33	He I	1.3	44
550–600		2.2	76
609.76	Mg X	0.53	17
629.73	O V	1.6	50
600–650		2.3	74
650–700		0.11	3.2
703.36	O III	0.36	10
700–750		0.49	13.4
765.15	N IV	0.17	4.4
770.41	Ne VIII	0.26	6.7
789.36§	O IV	0.68	10.8
750–800		1.8	46
800–850		1.5	35
850–900		3.5	78
900–950		3.3	71
977.02	C III	4.4	89
950–1000		6.0	121
1025.72	H I	3.5	68
1031.91	O VI	2.1	40
1000–1050		8.1	156
1050–1100		2.9	52
1100–1150		0.91	16
1150–1200		4.4	74
1215.67	H I	251	4100
1200–1250		259	4200
1250–1300		4.1	64
1302.17	O I	1.10	17
1304.86	O I	1.13	17
1306.03	O I	1.23	19
1334.53	C II	1.8	27
1335.70	C II	2.5	37
1300–1350		12.4	186
1393.76	Si IV	1.3	19
1350–1400		7.4	107
1402.77	Si IV	0.91	12.9
1400–1450		10.4	145
1450–1500		16.2	218
1548.19	C IV	3.8	49
1500–1550		29	381
1550.77	C IV	1.9	25
1561.0§	C I	2.5	32
1550–1600		40	503
1600–1650		56	681
1657.2§	C I	8.5	102

Table 1c (continued)

Wavelength, Å	Ion	Intensity incident on Earth 10^9 ph. cm^{-2} s^{-1}	10^{-3} erg cm^{-2} s^{-1}
1650–1700		130	1540
1700–1750		225	2590
1750–1800		357	3990
1808.01	Si II	9.2	101
1816.93		14.2	155
1816.45		5.5	60
1800–1850		604	6570
1850–1900		777	8230
1900–1940		829	8580

From HEROUX and HINTEREGGER (1978).
§ From averaged weighted energy levels of the multiplet. Integrated intensity for the multiplet is given.

The full calculation of the photoelectron flux as a function of energy is tedious and for many problems it is adequate to scale the photoionization production rate to simulate the additional impact source. Currently, some differences exist between various groups concerning the values that should be adopted for these scaling factors. OPPENHEIMER *et al.* (1977a), using the electron impact cross sections compiled by G. VICTOR (which comprise part of the AE on line data base), derived the values given in Table 2. Also shown in Table 2 are values that have been adopted by D. TORR and TORR (1978). Their lower values for O^+ are based on airglow observations of $O^+(^2D–^2P)$ 7320 Å emission in the aurora which are significantly smaller than theoretical values derived using the AE cross sections compiled by G. VICTOR. Figure 3 shows the 7320 Å auroral results of SWENSON (1976) and HAYS *et al.* (1975). They used a combination of high altitude satellite measurements made with AE and low altitude rocket measurements made with the Michigan Airglow Payload to demonstrate that quenching could not account for the low observed 7320 Å intensities. The effect of quenching at 220 km is small compared with 120 km. Thus, the emission could only be uniformly reduced to match the measurements at both low and high altitudes if the source function is reduced. Whether the reason for this is due to a low cross section has not yet been established. RUSCH *et al.* (1976, 1977a) studied the 7320 Å dayglow on AE and found that the emission is consistent with the measured EUV fluxes of HEROUX and HINTEREGGER (1978) if the photoelectron source is negligible. MERIWETHER *et al.* (1978) have drawn the same conclusion from ground based observations of the 7320 Å emission. In the face of this conflict TORR and TORR (1978a) adopted intermediate values for electron impact O^+

Table 2. Unattenuated photoionization frequencies (s^{-1})

$O+h\nu\rightarrow O^+(^4S)+e$	1.39×10^{-7}*	OPPENHEIMER *et al.* (1977a)
$O+h\nu\rightarrow O^+(^2D)+e$	9.6×10^{-8}*	OPPENHEIMER *et al.* (1977a)
$O+h\nu\rightarrow O^+(^2P)+e$	5.6×10^{-8}*	OPPENHEIMER *et al.* (1977a)
$N_2+h\nu\rightarrow N_2^++e$	3.1×10^{-7}*	OPPENHEIMER *et al.* (1976)
$N_2+h\nu\rightarrow N^++N+e$	1×10^{-7}	OPPENHEIMER *et al.* (1977a)
$N_2+h\nu\rightarrow N^+(^1S)+e$	3×10^{-9}	BURNSIDE *et al.* (1978)
$O_2+h\nu\rightarrow O^++O+e$	9.2×10^{-8}*	OPPENHEIMER *et al.* (1977a)
$O_2+h\nu\rightarrow O_2^+(X^2\pi_g)+e$	2.4×10^{-7}*	OPPENHEIMER *et al.* (1977a)
$O_2+h\nu\rightarrow O_2^+(a^4\pi_u)+e$	1.6×10^{-7}*	OPPENHEIMER *et al.* (1977a)
$N+h\nu\rightarrow N^++e$	1.9×10^{-7}	D. TORR *et al.* (1974)
$He+h\nu\rightarrow He^++e$	6.8×10^{-8}	OPPENHEIMER *et al.* (1978)
$O^++h\nu\rightarrow O^{2+}+e$	8.7×10^{-8}	BREIG *et al.* (1977)

* These rates for O^+ production include production by relaxation of excited states of O^+ produced in inner shell ionizations. Rates for all species include ionization by photons produced by these relaxation processes. Rates for N_2^+, $O_2^+(^2\pi)$ and $O_2^+(^4\pi)$ include ionization into excited states followed by cascading.

Note: These ionization frequencies update the cross sections given in Table 1 and can be used to scale the latter.

Table 2*. Effective photoelectron impact ionization rates

(i) OPPENHEIMER *et al.* (1977)

	Percentage of the EUV production rate	
	150 km	250 km
$O+e \rightarrow O^+(^4S)+2e$	18	25
$O+e \rightarrow O^+(^2D)+2e$	35	48
$O+e \rightarrow O^+(^2P)+2e$	33	45
$N_2+e \rightarrow N_2^+ +2e$	19	30

(ii) D. TORR and TORR (1978)

$O+e \rightarrow O^+(^4S)+2e$	15–30
$O+e \rightarrow O^+(^4D)+2e$	15–30
$O+e \rightarrow O^+(^2P)+2e$	15
$O_2+e \rightarrow O_2^+ +2e$	30
$N_2+e \rightarrow N_2^+ +2e$	30

* These values are meant to be typical. Actual values depend upon atmospheric composition and fractional ionization.

production rates. They used the largest impact ionization rate that is consistent (within the experimental error limits) with 7320 Å auroral and airglow measurements. The value of 45% given by OPPENHEIMER *et al.* (1977a) for the unattenuated

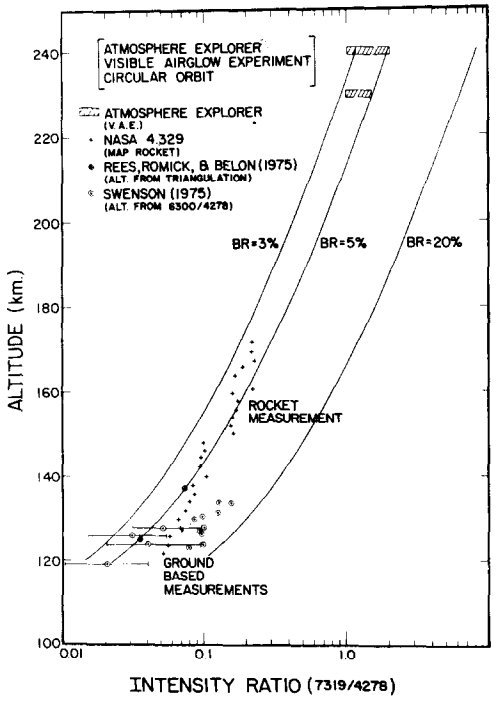

Fig. 3. The ratio of the surface brightness of 7320 Å to 4278 Å emissions as a function of altitude in the aurora from HAYS *et al.* (1975). (The reference to REES, REMICK and BELON (1975) was cited by HAYS *et al.*, 1975.)

impact fraction of the $O^+(^2P)$ source function requires significantly different quenching process than those obtained for a 15% fractional ionization rate. TORR and ORSINI (1978) have shown that a large source of $O^+(^2D)$ ions presents serious problems in interpreting measurements of N_2^+. According to photochemical results reviewed by TORR and TORR (1979a) the theoretical photoelectron ionization rates for $O^+(^2P)$ given by OPPENHEIMER *et al.* (1977a) are too high by up to a factor of 3. The theoretical photoelectron fluxes in turn are a factor of 2 to 3 lower than the measured fluxes of PETERSEN *et al.* (1977). If the latter are correct, a significant revision of our understanding of the chemistry of $O^+(^2P)$ and several other species will be required.

To complete the discussion on sources of ionization in the thermosphere we have included a discussion of recent results on various kinds of charged particle sources at mid-latitudes.

2.3 *Nocturnal sources of ionization*

2.3.1 *EUV radiation.* DONAHUE (1968) pointed out that the presence of an $[NO^+]$ peak at night implies a nighttime ionization source. A number of authors have suggested potentially important photoionization sources. Proposed radiation sources include HI Lyα and Lyβ, HeI 584 and HeII 304 Å. These emissions originate from solar radiation that has been resonantly scattered through the terrestrial atmosphere from the day-to-night sector. Extraterrestrial sources can also be significant. STROBEL *et al.* (1974) present plots of the scattered fluxes as a function of altitude and

zenith angle. These were computed from multiple scattering models and are normalized to or are consistent with direct measurements of the EUV emissions. STROBEL *et al.* (1974) find that the production rate at 150 km is $\sim 0.2\,cm^{-3}\,s^{-1}$ and $0.05\,cm^{-3}\,s^{-1}$ for O_2^+ and NO^+, respectively, due to resonantly scattered hydrogen geocorona. The extraterrestrial source of O_2^+ is about a factor of 2 lower. It is negligible for NO^+. The latter and scattered Lyβ form the dominant EUV sources of nocturnal ionization.

2.3.2 *Charged and neutral particle fluxes.*

(a) *Electrons and protons.* The question of whether there is a significant source of corpuscular radiation at night at middle latitudes has been controversial for over a decade (PAULIKAS, 1975). The literature abounds with many one-of-a-kind measurements which are difficult to explain. However, recent observations by the AE satellites have placed upper limits on average low- and mid-latitude electron and proton fluxes as a function of latitude and local time (i.e. day or night). Daytime fluxes are negligible sources of ionization at mid-latitudes. Figure 4 from D. TORR *et al.* (1976a) shows the total energy flux between 250 and 350 km as a function of invariant latitude as measured by the low energy electron experiment on AE-C (R. HOFFMAN *et al.*, 1973). The average electron flux at mid-latitudes at night was found to be $\sim(1\text{–}5)\times 10^{-4}\,erg\,cm^{-2}\,s^{-1}$. Recent unpublished work indicates values closer to $1\times 10^{-4}\,erg\,cm^{-2}\,s^{-1}$. The proton flux is about a factor of 2 lower. Measurements of the nocturnal N_2^+ 3914 Å emission by MERIWETHER and WALKER (1977, 1978) also support the lower particle fluxes, since the emission is consistent with production of N_2^+ by scattered EUV radiation. The results of D. TORR *et al.* (1976a) show that the particle energy flux may increase by more than an order of magnitude at times of high *Kp*. MERIWETHER and WALKER (1978) have reported an enhancement of N_2^+ emission during large magnetic disturbances. Simultaneous measurements of the N_2^+ rotational temperature suggest that the emission arises primarily from the *D*-region. It might, however, be difficult to deconvolve an *F*-region component from the higher energy fluxes which also increase during magnetically disturbed periods. D. TORR *et al.* (1976a) estimated that the low energy component should produce about 0.3–10 ions $cm^{-3}\,s^{-1}$ at the base of the *F*-region at mid-latitudes at night.

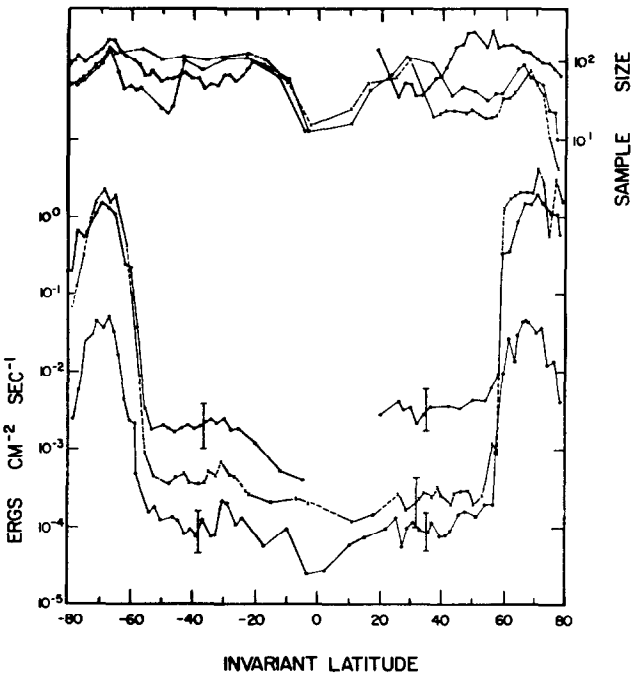

Fig. 4. The total energy flux between 250 and 300 km altitude as a function of invariant latitude: (O——●) electrons, daytime; (—x—) electrons, nighttime; (O——O) protons, nighttime. The three uppermost curves show the sample size for each invariant latitude bin (D. TORR *et al.*, 1976a).

(b) *Ring current particles.* TINSLEY (1978) has reported the detection of O^+, H, and He^+ emissions at low latitudes at night. He attributes the emissions to excitation by energetic neutrals produced at several Earth radii by charge exchange of ring current ions. Detailed calculations of this process were originally carried out by PRÖLSS (1975). The associated ionization in the *E*-region can be an order of a magnitude larger than ambient nighttime levels. TINSLEY (1978) estimates that since the energy input into the ring current is an order of magnitude more than the input into particle precipitation or Joule heating in auroral zones, the integrated low latitude energy input due to the precipitation of ring current particles is comparable to that of particle precipitation in the polar aurora. Although the energy flux is significantly smaller, the direct energy input into the low latitude thermosphere during larger storms is comparable with that carried by winds and waves from high latitudes.

(c) *Heavy ion precipitation.* SHARP *et al.* (1976) have reported large energy fluxes of heavy ions at middle latitudes. The peak energy deposition due to the precipitating ions is comparable with that due to precipitating ring current particles.

M. TORR *et al.* (1974) calculated the energy deposition rate due to precipitating O^+ ions together with estimates of heat input, excitation and ionization rates. Their results indicated significant heating due to momentum transfer from the fast oxygen neutrals which are produced by charge exchange of the incident O^+ ions.

The results also indicated that precipitation of fast O^+ ions results in a large ($>10^7\,cm^{-2}\,s^{-1}$) neutral oxygen escape flux. An interesting aspect of the phenomenon is that it appears to be potentially self sustaining. The outward flowing neutrals enter ballistic orbits and may be re-ionized and accelerated back into the atmosphere to produce a fresh flux of escaping neutrals.

3. MAJOR ION CHEMISTRY

3.1 *Introduction*

Figure 2 depicts the main chemical processes that govern the balance of ionization in the thermosphere. Ionization of O and N_2 by photons and photoelectrons constitute the major sources of ionization. Photoionization of O_2 is a minor source of O_2^+. Fifty-two percent of the O^+ ions are produced in metastable states (OPPENHEIMER *et al.*, 1977a), of which a significant fraction (which varies with altitude and season) is transformed into N_2^+ through charge exchange with N_2. In the *F*2-layer most of the $O^+(^4S)$ is converted into NO^+. At *E*-region heights most of the $O^+(^4S)$ is converted into O_2^+. The conversion of O_2^+ into NO^+ through ion atom interchange with N can be a significant low altitude loss process for O_2^+, especially at night. Ion atom interchange of N_2^+ with O accounts for the bulk of the loss of N_2^+ ions produced in the ionosphere. Recombination is an important high altitude loss process for N_2^+ ions. Recombination of NO^+ is the main sink for thermospheric ionization.

The processes shown in Fig. 2 have been studied quantitatively using AE data and the reaction rates and branching ratios indicated have all been determined. In carrying out these studies, the large dynamic range that occurs in nature for most aeronomic parameters has been used to select data for conditions that emphasize processes to be studied, and minimize others. Data can be sorted or analyzed as a function of any measured parameter such as temperature (T_e, T_i or T_n), density, etc. In many cases it has been possible to reduce the chemistry of a constituent to one source and one sink by appropriate data selection. Generally the circumstances chosen for study include one known and one unknown process. This allows the unknown rate coefficient to be unambiguously determined. In some cases it is useful to study two processes where the rate coefficients are both unknown in order to determine the ratio of rate coefficients.

We describe in subsequent sections the quantitative determination of the rate coefficients of the processes shown in Fig. 2.

3.2 *Determination of the* NO^+ *recombination rate coefficient*

The nitric oxide ion NO^+ is the main ionic species in the lower thermosphere. Since it has the lowest heat of formation of the five major thermospheric ions, it is removed chemically by recombination only and it is produced by reactions involving all other ions. An accurate knowledge of nitrogen atom production depends strongly on the rate of recombination of NO^+. However, a controversy currently exists concerning the electron temperature dependence of this rate coefficient. We use the aeronomic determination of this parameter to illustrate the general approach that has been used to determine many other rate coefficients.

The NO^+ recombination rate coefficient has been measured in the laboratory by two different techniques. The most recent measurement was made by HUANG *et al.* (1975) who used a microwave-afterglow spectrometer apparatus. They found that

the recombination rate, α_1, varied as $T_e^{-0.37}$. The second group, WALLS and DUNN (1974), used an ion trap to store the ions prior to recombination. They found that α_1 varied as $T_e^{-0.83}$. WALLS and DUNN (1974) effectively normalized their results to those of MEHR and BIONDI (1969) by using the well established measurements on O_2^+ recombination at 2000 K to calibrate their instrument. This calibration does not depend significantly on ion species.

The difference in temperature dependence derived by the two groups results in a difference of a factor of 2 in α_1 at 2000 K, i.e. for typical daytime F-region electron temperatures. Such an uncertainty seriously affects the calculation of the production of $N(^2D)$ atoms and hence our knowledge of the concentration of odd nitrogen species in the thermosphere.

It has been difficult to find an explanation for the discrepancy in the laboratory measurements. The only obvious difference lies in the vibrational state of the NO^+ ions in each experiment. In the microwave-afterglow apparatus the ions are believed to be produced mainly in the $v=1$ and $v=2$ states of the ground electronic state of NO^+. WALLS and DUNN (1974), on the other hand, store their ions for long enough to ensure that they recombine principally in the $v=0$ state. Since vibrational lifetimes of NO^+ are of the order of tens of milliseconds (TAKANAYAGI, 1964), it seems reasonable to expect that the results of WALLS and DUNN (1974) will correspond more closely to actual conditions in the upper atmosphere where the chemical lifetime of NO^+ is of the order of tens to hundreds of seconds. However, theoretical studies of the physics of the recombination process suggest that the rate coefficient should decrease for $v>0$ (MICHELS, 1974).

The question as to which rate should be used in the atmosphere was resolved by D. TORR *et al.* (1976b). They used the photochemistry of NO^+ at night to determine α_1 from a sample of ~3000 measurements. They constrained their data to that taken above 240 km at mid-latitudes, thus reducing the chemistry to one source and one sink, namely the reactions

$$O^+ + N_2 \xrightarrow{k_1} NO^+ + O, \tag{3.1}$$

and

$$NO^+ + e \xrightarrow{\alpha_1} N + O, \tag{3.2}$$

so that α_1 is given by

$$\alpha_1 = \frac{k_1[O^+][N_2]}{[NO^+][N_e]}. \tag{3.3}$$

For the bulk of their data the ion temperature lay close to 750 K, thus eliminating the effect of a temperature dependence in k_1 on the results. This analysis was later refined by M. TORR *et al.* (1977b) and M. TORR and TORR (1979a) using the rate coefficient for the $O^+ + N_2$ reaction discussed in Section 3.3.

Figure 5 shows the results obtained by M. TORR and TORR (1979a), where an analytical fit to the data is given by the exponential limits of the equation

$$\alpha_1 = (4.3 \pm 1) \times 10^{-7} (T_e/300)^{-0.83^{+0.16}_{-0.08}} \text{ cm}^3\text{s}^{-1}. \tag{3.4}$$

The results of MEHR and BIONDI (1969) are also shown.

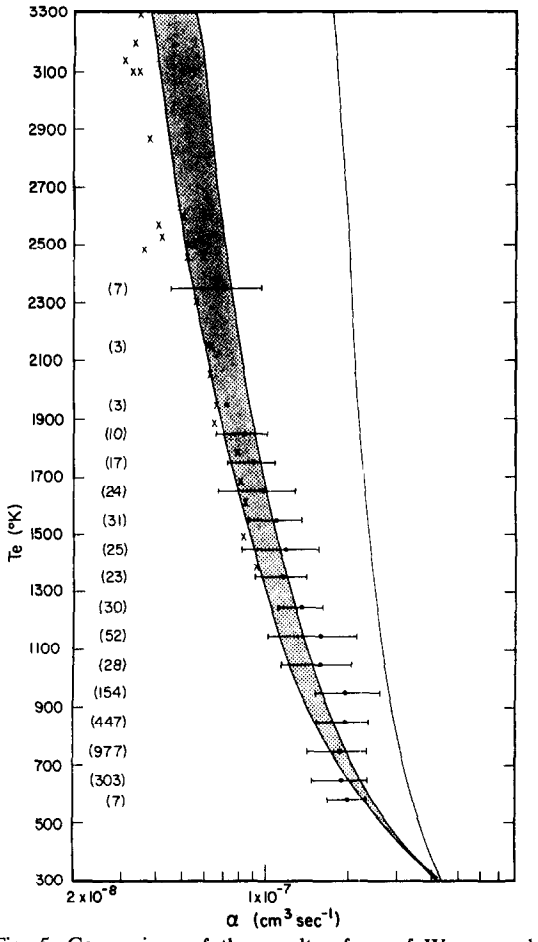

Fig. 5. Comparison of the results of α_1 of WALLS and DUNN (1974) (shaded curve) and MEHR and BIONDI (1969) with the earlier AE results of M. TORR *et al.* (1977b) (|—●—|) and the most recent AE results of M. TORR and TORR (1979a) (×).

The crosses represent the most recent results which increase the range in electron temperature further (TORR and TORR, 1979a). This is in excellent agreement with the temperature dependence of WALLS and DUNN (1974). The absolute values which are based on the O_2^+ recombination rate measurements of MEHR and BIONDI (1969) yield values for k_1 which are in excellent agreement with the laboratory results of ALBRITTON *et al.* (1977) (see Section 3.3).

We address below the question of possible sources of error in analyses of the type described above. Problems that might arise in atmospheric determinations of rate coefficients stem largely from the fact that some basic knowledge of the photochemistry being studied is assumed. The possibility always exists that a reaction might have been overlooked. In particular, this would be true in the case of a 'hidden reaction', i.e. one whose effects might not be readily detectable because of cancelling processes. An example would be a reversible process providing both a source and sink for the same constituent.

M. BIONDI (private communication, 1978) has brought to our attention the fact that the temperature dependence of α_1 determined by WALLS and DUNN (1974) depends rather critically on a single point at the low temperature end, where the measurement is difficult to make using the ion storage technique. Because of this uncertainty, and the unresolved controversy in the laboratory results we have searched for possible sources of error in the above analysis.

M. BIONDI (private communication, 1978) suggested that the mechanism

$$N(^2D) + O \xrightarrow{k_{2a}} NO^+ + e - 0.37\,\text{eV}, \quad (3.5a)$$

might be an additional source of NO^+. This process has been studied experimentally by ZIPF (1978). For cases where $N(^2D)$ atoms are produced with sufficient kinetic energy, such as in the aurora, (3.5a) will constitute an important source of NO^+ ions. However, in the nocturnal mid-latitude ionosphere the only significant source of $N(^2D)$ atoms is recombination of NO^+. If we include reaction (3.5a) in the NO^+ chemistry then (3.4) for α_1 is modified to:

$$\alpha_{NEW} = \alpha_1(k_{2a} + k_{2b})/k_{2b}, \quad (3.5b)$$

where k_{2b} is rate coefficient for O quenching of $N(^2D)$. Clearly inclusion of (3.5a) does not alter the temperature dependence of α_1. The results of M. TORR and TORR (1979a) demonstrate a dependence of the form T_e^{-1} rather than $T_e^{-0.4}$. Thus (3.5a) is not an acceptable explanation for the discrepancy between the AE results for α_1 and the measurements of HUANG *et al.* (1975).

Another difficulty experienced in analyses conducted with a multi-instrument system involves the estimation of absolute errors. Three main approaches have been adopted in assessing these in the AE results.

3.2.1 *Duplication of measurements and inter calibration with ground based facilities.* In designing the AE payloads provision was made to duplicate the measurements of most of the important aeronomic parameters by using two instruments employing different measuring techniques. In each case where two instruments have measured the same parameters, detailed comparisons have been made between the results obtained. During the period August 1974–February 1975 comparisons were made between measurements made by the magnetic ion mass spectrometer (MIMS) (J. HOFFMAN *et al.*, 1973) and the Bennett ion mass spectrometer (BIMS) (BRINTON *et al.*, 1973). These measurements showed that BIMS and MIMS agreed to within ±25% for the major ion densities. The electron density and total ion concentration were measured by the cylindrical electrostatic probe (CEP) (BRACE *et al.*, 1973) and the retarding potential analyzer (RPA) (HANSON *et al.*, 1973). These measurements agreed to within ±10%. The RPA ion temperatures and the CEP electron temperatures have been compared with incoherent scatter measurements and are believed to be accurate to within ±5% (BENSON *et al.*, 1977). Airglow measurements made by the Visible Airglow Experiment (VAE) (HAYS *et al.*, 1973) were compared with a network of ground based stations, and despite the difficulties involved with such intercomparisons, agreement with well calibrated ground stations amounted to ±30% (M. TORR *et al.*, 1977a).

The N_2 density was measured by the open source mass spectrometer (OSS) (NIER *et al.*, 1973) and by the neutral atmosphere composition experiment (NACE) (PELZ *et al.*, 1973). The NACE measurements were compared with simultaneous measurements of neutral densities made by OSS. The O and N_2 densities measured by the two instruments were found to agree to within ±10% (G. R. CARIGNAN, private communication, 1976). Neutral temperatures measured by the neutral atmosphere temperature instrument (NATE) (SPENCER *et al.*, 1973) were compared with those obtained from neutral density scale heights and other techniques (cf. HEDIN *et al.*, 1976). The agreement was good.

3.2.2 *Different photochemical studies of the same rate coefficient.* A second means of checking the reliability of measurements is provided by the constraints imposed by studying the same reaction under a different set of photochemical conditions, i.e. with different related source or sink terms. OPPENHEIMER *et al.* (1977b) have repeated the determination of the NO^+ recombination rate using measurements taken during the daytime. In the sunlit ionosphere the reaction

$$N_2^+ + O \rightarrow NO^+ + N,$$

must be included in the chemistry.

The analysis of the NO^+ recombination process was the first in a series of quantitative rate coefficient determinations made using the AE data. It has been our experience with the AE data that an inconsistency in a single major parameter can be readily detected when large samples (thousands) of data are analyzed. The values derived for several ionospheric reactions have subsequently been incorporated into a comprehensive general diurnally varying photochemical model of the ionosphere, where self-consistent results have been obtained for all major ionic species (D. TORR *et al.*, 1979). This is discussed further in Section 3.5.

3.2.3 *Comparison with laboratory results.* Finally, comparisons have been made whenever possible with laboratory results, and in the large majority of cases excellent agreement has been achieved. The two notable exceptions are the NO^+ recombination, and the recombination of N_2^+ where a missing process was identified in the ion chemistry used for the AE analysis. This is discussed further in Section 3.5.

Because no quantitative assessment can be readily made of the absolute accuracy of the rate coefficients determined from the AE data, the 'center of gravity' approach has been adopted in the application of the results derived in one situation to another situation, i.e. the mean value is used without further error analysis. The effect of errors in the input rate coefficients will have the effect of increasing the standard deviation on the resultant rate coefficient thus determined. Error bars, unless otherwise stated, indicate the standard deviation arising from the statistical analysis, and should not be taken to mean absolute error.

However, because of the excellent self consistency obtained from one ion species to another, and because of the good agreement with laboratory results in general, the standard deviations can, for most cases, be regarded as 'error bars'.

3.3 *Sources of* NO^+ *ions*

As indicated in Fig. 1 the major sources of NO^+ at altitudes above 155 km are the reactions

$$O^+ + N_2 \xrightarrow{k_3} NO^+ + N, \tag{3.6}$$

$$N_2^+ + O \xrightarrow{k_4} NO^+ + N. \tag{3.7}$$

Above about 300 km the reaction

$$N^+ + O_2 \xrightarrow{k_5} NO^+ + O \tag{3.8}$$

becomes non-negligible, and at altitudes below 200 km reactions

$$O_2^+ + N \xrightarrow{k_6} NO^+ + O, \tag{3.9}$$

$$O_2^+ + NO \xrightarrow{k_7} NO^+ + O_2, \tag{3.10}$$

are potentially important sources of NO^+. The latter two processes are discussed in Section 3.4.

3.3.1 $N_2 + O \rightarrow NO^+ + N$. D. TORR *et al.* (1977) studied the $N_2^+ + O$ reaction using data taken at altitudes below 200 km. Under these conditions the chemistry of N_2^+ which is discussed in Section 3.5 is simple, and the N_2^+ concentration is given by

$$Q_{N_2}/k_4[O], \tag{3.11}$$

where Q_{N_2} represents all the photoelectron and photoionization and charge exchange sources of N_2^+ referred to in Section 3.5. D. TORR *et al.* (1977) searched through all the AE-C data taken at altitudes below 200 km for mid- and low-latitude daytime conditions and calculated values of k_4 from (3.11) as a function of ion temperature. The agreement with the laboratory results of MCFARLAND *et al.* (1974) is excellent at 600 K. At higher temperatures there is a small but systematic divergence between the AE and laboratory results. D. TORR *et al.* (1977) attributed this to their neglect of recombination which is a small term below 200 km. D. TORR *et al.* (1978) have subsequently shown that not all the $O^+(^2D)$ ions charge exchange to form N_2^+ at low altitudes. Some are quenched and some charge exchange with O_2. The latter process, however, only becomes a significant sink for $O^+(^2D)$ at altitudes below 160 km. The bulk of the data analyzed by D. TORR *et al.* (1977) was taken between 160 km and 200 km where (3.11) is valid.

3.3.2 $O^+ + N_2 \xrightarrow{k_3} NO^+ + N$. Using nocturnal measurements when (3.7) is a negligible source of NO^+, and daytime measurements when it is a

major source, M TORR *et al.* (1977b) determined the temperature dependence of k_3 for altitudes between 240 and 340 km [in order to eliminate reactions (3.8) to (3.10)]. The NO^+ recombination rate discussed in the previous section was used in the analysis. We remind the reader that in the recombination rate determination, data were chosen to keep the ion temperature constant at ~750 K. The derivations of the temperature dependences of α, and k_3 are therefore independent.

Figure 6 shows k_3 as a function of ion temperature as determined from the AE data. Also shown in Fig. 6 are the calculations of k_3 of M. TORR *et al.* (1977b) as a function of ion temperature using the cross sections of ALBRITTON *et al.* (1977) as described by ST-MAURICE and TORR (1978). Curve 1 represents a non-drifting Maxwellian ion velocity distribution; curve 2 a drifting Maxwellian in an N_2 atmosphere and curve 3 a drifting Maxwellian in an O atmosphere. The bars on the curves represent variations that would arise as a result of the diurnal variation of T_n, since T_i is related to T_n and u by the expression

$$3kT_i = 3kT_n + m_b u^2, \tag{3.12}$$

where m_b is the mass of the buffer gas and u is the relative drift velocity.

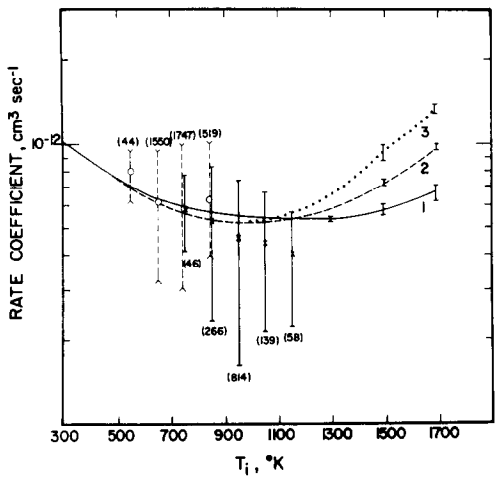

Fig. 6. The rate coefficient k_1 as a function of ion temperature. The points with full standard deviation bars are the AE determination from data measured during the day, and the dashed bars are the nighttime determination. The curves represent the calculation of k_3 for various ionospheric conditions using the cross sections of ALBRITTON *et al.* (1977); curve 1 is the non-drifting Maxwellian ion velocity distribution, curve 2 is the drifting Maxwellian distribution in an N_2 atmosphere, and curve 3 is the drifting Maxwellian distribution in an O atmosphere (M. TORR *et al.*, 1977).

The results presented in Fig. 6 indicate how the rate coefficient will vary in the atmosphere as a function of T_i as a result of variations in the relative velocity distributions of the reactants. In Fig. 7 we show the same theoretical results plotted as a function of effective temperature defined by

$$T_{eff} = \frac{2}{3k} KE_{cm}, \tag{3.13}$$

where

$$KE_{cm} = \left(\frac{m_n}{m_i + m_n} + \frac{m_i u^2}{2} + \frac{3kT_i}{2} - \frac{3kT_n}{2}\right) + \frac{3kT_n}{2}, \tag{3.14}$$

and m_i and m_n are the ion and neutral masses, respectively. Also shown in Fig. 7 are values calculated from an expression given by MCFARLAND *et al.* (1973) for comparison, since these have been used extensively in the literature. The MCFARLAND curves represent an empirical fit to the earlier laboratory results of several groups (see M. TORR *et al.*, 1977b). The AE results agree with curve A derived from the most recent laboratory measurements of ALBRITTON *et al.* (1977). Curve B illustrates how the rate coefficient is sensitive to the 'buffer' gas for a drifting Maxwellian velocity distribution.

ST-MAURICE and TORR (1978) have carried out a polynomial fit to the results shown in Fig. 7. They find that k_3 can be approximated to within ±15% by the expression

$$k_3 = 1.533\times10^{-12} - 5.92\times10^{-13}(T_{eff}/300) + 8.6 \times 10^{-14}(T_{eff}/300)^2 \quad \text{for} \quad 300 \le T_{eff} \le 1700\ \text{K}, \tag{3.15a}$$

and

$$k_3 = 2.73\times10^{-12} - 1.155\times10^{-12}(T_{eff}/300) + 1.483 \times 10^{-13}(T_{eff}/300)^2 \quad \text{for} \quad 1700 < T_{eff} < 6000\ \text{K}. \tag{3.15b}$$

From their studies of variations in the velocity distribution for a variety of atmospheric situations ST-MAURICE and TORR (1978) drew the following conclusions.

(1) The $O^+ + N$ rate coefficient is controlled largely by the population in the tail of the relative speed distribution owing to a strong increase in the cross section, $\sigma(v)$ at high relative speeds.

(2) Rate coefficients in the laboratory and in the thermosphere are approximately the same for the same value of KE_{cm}, if a thermal-equilibrium apparatus such as a static or flowing afterglow system is used in the laboratory.

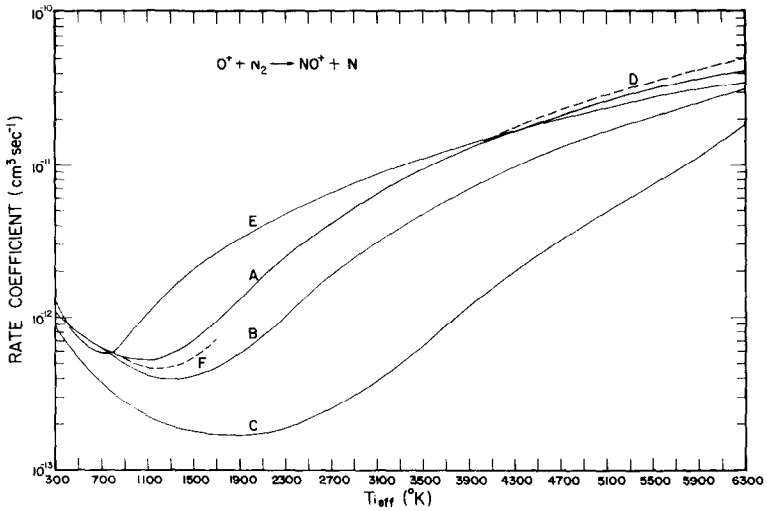

Fig. 7. Rate coefficient as a function of T_{eff} for the $O^+ + N_2$ reaction, under various assumptions. Curve A is the rate coefficient at mid-latitude and for displaced bi-Maxwellian ion velocity distributions in convecting high-latitude regions; curve B, displaced Maxwellian in a helium buffer; curve C, (see ST-MAURICE and TORR, 1978); curve D, same as curve A but with highly non-Maxwellian ion velocity distributions; curve E, rate given by MCFARLAND *et al.* (1973); and curve F, displaced Maxwellian in the topside ionosphere under periods of fast convection. Details on the various assumptions are given by ST-MAURICE and TORR (1978).

(3) The rate coefficients are in general not the same in the atmosphere as in drift-tube experiments, although for O^+ in a helium buffer the difference is about 25% or less.

3.4 O_2^+ *chemistry*

There are three processes which result in the destruction of O_2^+ ions in the ionosphere at *E*- and *F*-region heights, namely recombination:

$$O_2^+ + e \xrightarrow{\alpha_2} O + O, \tag{3.16}$$

and charge exchange with N and NO (reactions 3.9 and 3.10, respectively). Recombination is the only significant loss process for O_2^+ during the day at altitudes above ~190 km. The rate coefficient is well established. There is excellent agreement between different laboratory measurements (e.g. MEHR and BIONDI, 1969; WALLS and DUNN, 1974), and D. TORR *et al.* (1976c) have confirmed that O_2^+ recombines at the same rate in the ionosphere as in the laboratory, namely

$$\alpha_2 = 1.6 \times 10^{-7} (T_e/300)^{-0.55}. \tag{3.17}$$

In the aeronomic determination of α_2 D. TORR *et al.* (1976c) analyzed AE data taken between 190 and 240 km for solar zenith angles less than 80°. Under these conditions the only significant source of O_2^+ is

$$O^+ + O_2 \xrightarrow{k_8} O_2^+ + O. \tag{3.18}$$

The reactions

$$O_2 + h\nu \longrightarrow O_2^+ + e,$$
$$O^+(^2D) + O_2 \xrightarrow{k_9} O_2^+ + O, \tag{3.19}$$
$$N^+ + O_2 \longrightarrow O_2^+ + N,$$

comprise less than 20% of the total O_2^+ source function over the above given altitude regime. Neglect of these minor sources is approximately compensated for by omitting loss reactions with odd nitrogen over the same altitude range.

Under these conditions the recombination rate coefficient α_2 is given by

$$\alpha_2 = \frac{k_8[O^+][O_2]}{[O_2^+][N_e]}. \tag{3.20}$$

In their determination of α_2 D. TORR *et al.* used the values of MCFARLAND *et al.* (1973) for k_8. Ionospheric values for k_8 have subsequently been calculated by ST-MAURICE and TORR (1978) from cross sections of ALBRITTON *et al.* (1977). The latter used laboratory measurements of k_8 to derive the cross sections as a function of energy. The results of ST-MAURICE and TORR (1978) are shown in Fig. 8. Also shown are the values of MCFARLAND *et al.* (1973) which were used for k_8 by TORR *et al.* (1976c) (curve E). At temperatures below 1900 K the ionosphere values for midlatitude conditions for k_8 (curve A) lie close to the results of

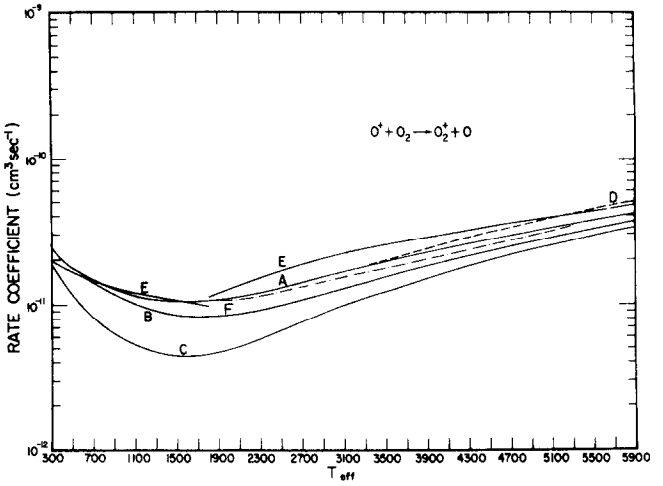

Fig. 8. Same as Fig. 7, but for the reaction $O^+ + O_2 \rightarrow O_2^+ + O$.

MCFARLAND *et al.* (1973). Therefore the new values for k_8 do not change the values for α_2 derived by TORR *et al.* (1976c) for the O_2^+ recombination rate coefficient.

A polynomial fit to the ionospheric rate coefficient k_8 as a function of T_{eff} is given by ST-MAURICE and TORR (1978).

$$k_8 = 2.82\times10^{-11} - 7.74\times10^{-12}(T_{eff}/300) + 1.073 \times 10^{-12}(T_{eff}/300)^2 - 5.17\times10^{-14}(T_{eff}/300)^3 + 9.65\times10^{-16}(T_{eff}/300)^4 \text{ for } 300 \le T_{eff} \le 6000 \text{ K}. \quad (3.21)$$

3.4.1 *The effect of reactions with* N and NO *on* O_2^+. Measurements of the 5200 Å $N(^4S-^2D)$ emission made by the visible airglow experiment on AE (HAYS *et al.*, 1973) led RUSCH *et al.* (1975a) to infer surprisingly high values for the concentration of atomic nitrogen in the thermosphere ($[N] > 10^7$ cm^{-3} at 200 km). These findings were confirmed soon thereafter by direct measurements of the N density at 400 km by the AE open source mass spectrometer (MAUERSBERGER *et al.*, 1975) ($[N] \approx 10^6$ cm^{-3} at 400 km). The chemistry of odd nitrogen in the thermosphere is treated in Section 4.2. In this section we discuss the effect of N densities of this magnitude on the chemistry of O_2^+.

Figure 9 (M. TORR *et al.*, 1975) shows a comparison of results obtained using the theory given above compared with nighttime AE measurements of O_2^+. The discrepancy shown was identified as being due to neglect of O_2^+ destruction by odd nitrogen (reactions 3.9 and 3.10). From the data shown in Fig. 9, M. TORR *et al.* (1975) deduced values of $\sim 10^7$ cm^{-3} at 200 km for [N] at night. The N density on orbit 3671 was probably enhanced by about a factor of 2 with respect to normal behavior, as the data were selected because of the clearly observable discrepancy. Analyzing daytime AE-C ion and neutral composition measurements D. TORR *et al.* (1976d) found that the N densities of RUSCH *et al.* (1975a) between 160 and 200 km were consistent with the measured O_2^+ concentrations. The high altitude measurements of MAUERSBERGER *et al.* (1975) which were made at low-latitudes could only be reconciled with the O_2^+ measurements near perigee (~160 km) if a strong latitude gradient in N exists between the equator and mid-latitudes, resulting in a decrease in concentration at ~160 km of a factor of 3. The measured O_2^+ concentrations place a limit of ~2–3 × 10^7 cm^{-3} on the N density at 160 km during daytime conditions. If the N density were to exceed

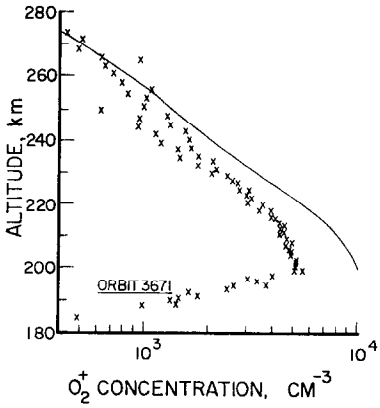

Fig. 9. Concentrations of O_2^+ as a function of altitude at night on AE-C orbit 3613 (15 October 1974, 0300 LT). The full line joins theoretical values ignoring $N(^4S)$ (M. TORR *et al.*, 1975); the crosses are MIMS measurements (J. HOFFMAN *et al.*, 1973).

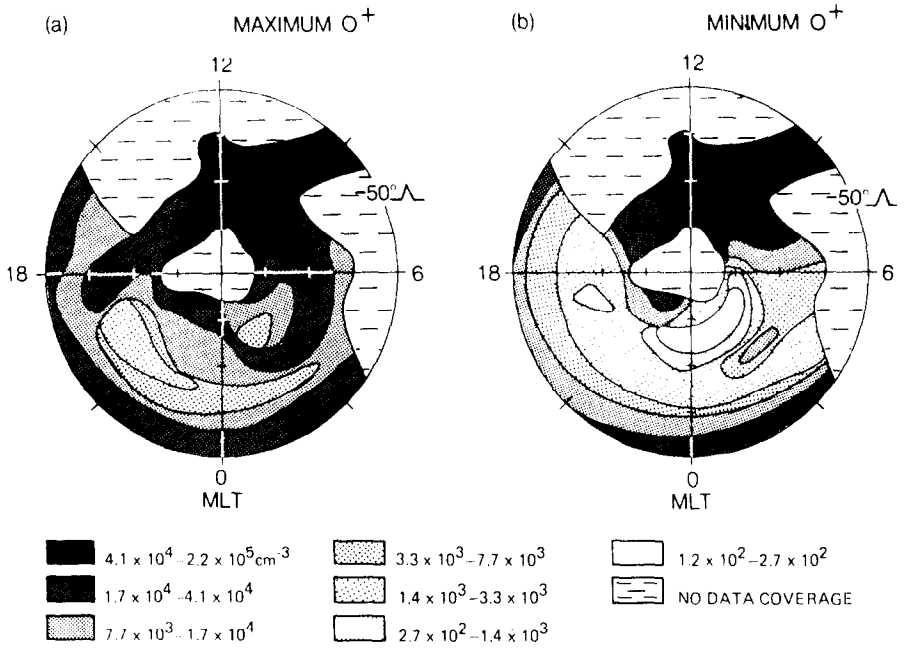

Fig. 10. Topographic maps of O^+ concentrations indicating for any MLT-A location, the maximum (a) and minimum (b) O^+ density measured at that point during the 100-day period comprising the database (BRINTON *et al.*, 1978).

this concentration a measurable decrease in $[O_2^+]$ would be observed at 160 km. Loss of O_2^+ due to NO amounts to about 30% at 160 km of that due to N, and is therefore of marginal importance over the altitude range covered by AE. At lower altitudes, and at high-latitudes reactions with NO have a major effect on ionospheric composition (cf. DONAHUE *et al.*, 1970; SHARP, 1978).

3.4.2 *Effects of atomic nitrogen at high latitudes.* Effects of odd nitrogen on the chemistry of the ionosphere at high-latitudes is complex and poorly understood. However, mapping of ion concentrations at high-latitudes at altitudes of ~300 km in winter by BRINTON *et al.* (1978) has revealed several interesting topographical ionic features which can be understood in terms of the O_2^+ and NO^+ chemistry discussed in the preceeding sections. Figure 10 shows a typical topographical map for O^+ derived by BRINTON *et al.* (1978) from AE data. The map shows a depletion of ionization on the eastward night side of the polar cap. Figure 11 identifies the dominant molecular ion in the vicinity of the ionization hole as NO^+. Figure 12 shows measurements made by AE-C on orbit 14,182. The trajectory passed through the ionization hole. The plots of ion concentrations show that in the hole O_2^+ decreases to below the threshold of detection. BRINTON *et al.* (1978) observed that the variations in O_2^+ correlated closely with those in O^+. NO^+, on the other hand, does not correlate well with variations in O^+, but with changes in T_e.

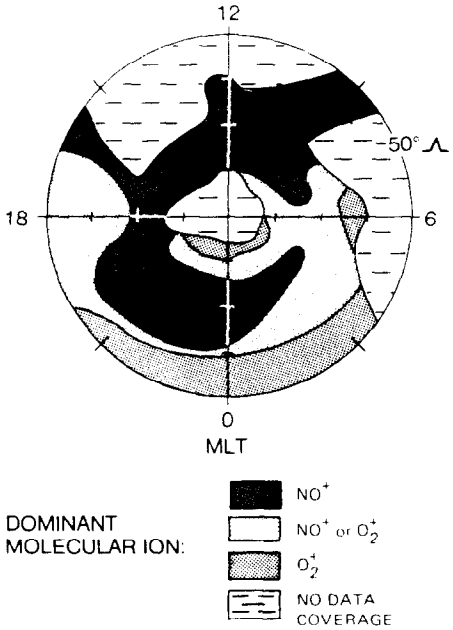

Fig. 11. Topographical map indicating regions at high-latitudes where NO^+ or O_2^+ was the dominant molecular ion (BRINTON *et al.*, 1978).

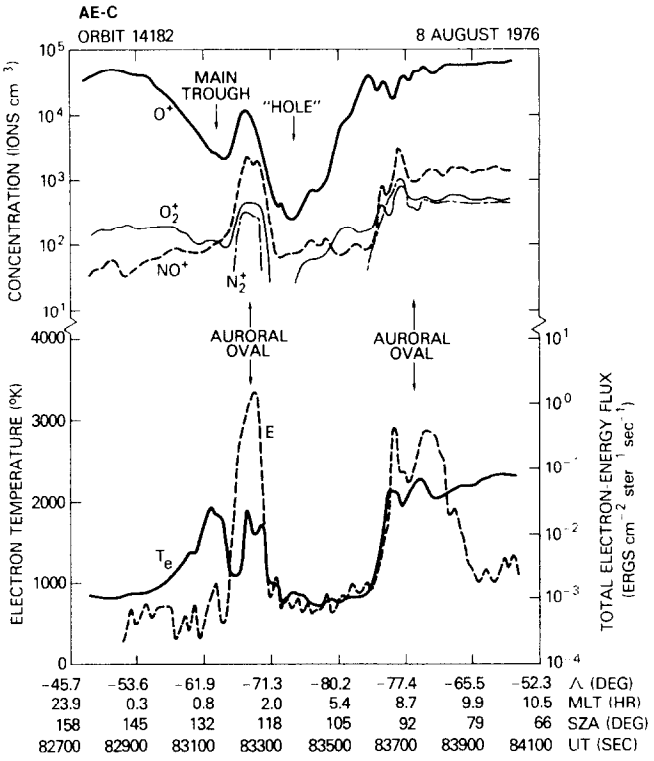

Fig. 12. Simultaneous measurements of ion composition, T_e, and energetic electron flux on AE-C orbit 14,182 through the winter F-region at southern high-latitudes. Prominent ionospheric features are indicated with arrows. (BRINTON *et al.*, 1978).

BRINTON *et al.* (1978) interpreted their observations in terms of the occurrence of long residence times over the polar cap caused by small drift velocities ($0.1\,\mathrm{km\,s^{-1}}$) in the anti-sunward direction. As a result of the absence of sources of ionization the electron density decays to a very low level. Under these conditions quasi-photochemical equilibrium is eventually reached (M. TORR and TORR, 1979a) and the concentrations of O_2^+ and NO^+ are given, respectively, by

$$[O_2^+]=\frac{k_8[O_2][O^+]}{k_6[N]}, \tag{3.22}$$

since $\alpha_2[N_e]\ll k_6[N]$ in the ionization hole, (BRINTON *et al.*, 1978): and

$$[NO^+]=\frac{k_3[N_2][O^+]}{\alpha_1[N_e]} \tag{3.23}$$

$$\approx 1.5\times10^{-4}[N_2]T_e^{0.85}, \tag{3.24}$$

since $[O^+]\approx[N_e]$ at 300 km altitude.

Equations (3.22) and (3.24) explain why O_2^+ covaries with O^+, and NO^+ with T_e.

The concentration of molecular ions in main ionospheric trough (which is shown in Figs. 11 and 12) exhibit similar dependences on N and T_e. The trough is observed to be deepest near dusk. The mechanism responsible for this behavior has been identified as the cancellation of plasma co-rotation by solar wind induced plasma convection velocities (SPIRO *et al.*, 1978). This results in long residence times in the dusk sector, which does not occur in the dawn sector. In contrast to NO^+, a minimum in O_2^+ density occurs between $-60°$ and $-70°$ invariant latitude after dusk, coincident with the deepest part of the main O^+ trough. Associated with these effects is a peak in T_e caused by energy transported downward from the protonosphere by heat conduction. The lower ion density in the trough causes reduced electron–ion cooling, thus permitting the downward-flowing protonospheric heat to be conducted deep into the F-region where it produces the observed T_e enhancement. The elevated NO^+ densities are caused by the elevated electron temperatures which decrease the recombination rate. The depleted O_2^+ is caused by loss with N.

The above simplified discussion of how purely chemical effects impact the behavior of the high-latitude ionosphere demonstrates how important it

is to have quantitative information on rate coefficients before we can understand the details of the processes discussed above.

Ionospheric chemistry also plays an important role in regimes which are dominated by dynamical effects. Several key rate coefficients are highly energy dependent (cf. Figs. 7 and 8 for the reactions $O^+ + N_2$ and $O^+ + O_2$) and increase significantly in the presence of drifts caused by high-latitude convection electric fields (SCHUNK *et al.*, 1976; BANKS *et al.*, 1974).

BRINTON *et al.* (1978) report observations of regions of localized O^+ depletions in the cusp region associated with corresponding molecular ion increases. These are attributed to enhanced reaction rates due to high speed plasma drifts. The rate coefficients k_3 and k_8 have been computed by ST-MAURICE and TORR (1978) for cases of high speed plasma drift where the relative velocity distributions of reactants may be highly non-Maxwellian (see curves D and F in Figs. 7 and 8). These results can be used to quantitatively model ion concentrations in regions of convective electric fields provided that the effective temperature (cf. 3.13, 3.14) is used in (3.15) and (3.21).

3.4.3 *The effects of reactions of metastable* O^+ *ions on* $[O_2^+]$. D. TORR *et al.* (1978) demonstrated that under conditions of enhanced molecular constituent densities at *F2*-layer altitudes the reaction

$$O^+(^2D) + O_2 \xrightarrow{k_{10}} O_2^+ + O, \qquad (3.25)$$

becomes an important, if not a major, source of O_2^+ ions. This happens because of a reduction in the O^+ concentration (and hence $[N_e]$) as a result of ion molecule interactions between $O^+(^4S)$ and N_2. The reduction in $[N_e]$ also leads to enhanced $O^+(^2D)$ densities as a result of a corresponding decrease in electron quenching (see Section 3.5 and Fig. 2). The enhanced N_2 densities and reduced electron densities result in reaction (3.25) exceeding the conventional major source of O_2^+, namely (3.18). D. TORR *et al.* (1978) show that under these conditions the ratio R of the sources of O_2^+ due to (3.25) to that due to (3.18) is given by

$$R \approx \frac{1}{4J}\frac{k_{10}k_3^2}{k_8k_{11}}\frac{[N_2]^2}{[O]}, \qquad (3.26)$$

where J is the photoionization frequency for $O^+(^4S)$, k_{11} is the $O^+(^2D)$ electron quenching rate coefficient (see Section 3.5). Equation 3.26 yields values between 0.1 and 1 for the range typical observed for the ratio $[N_2]^2/[O]$ at 300 km. The rate coefficient k_{10} was found to be $1 \pm 0.6 \times 10^{-9}$ cm^3 s^{-1}.

D. TORR *et al.* (1979) also examined the low altitude case where $O^+(^2D)$ ions were believed to be lost primarily in reactions with N_2. In this case, including reaction (3.25), R is given by

$$R \approx \frac{[O_2]}{0.25[N_2] + [O_2]}. \qquad (3.27)$$

This result shows that reaction (3.25) is a significant sink for $O^+(^2D)$ ions in the lower *F*- and *E*-regions, as well as constituting a detectable source of O_2^+. In the altitude range 190–240 km there is a transition from the high altitude to low altitude chemistry where charge exchange of $O^+(^2D)$ with O_2 constitutes less than 20% of the total source of O_2^+. Below 200 km, reaction (3.25) begins to compete as a sink for $O^+(^2D)$ ions. For example at 200 km the $[O_2]/[N_2]$ ratio ≈ 0.1 and $R \approx 0.3$, and reaction (3.25) is 40% of reaction (3.18). At 120 km $[O_2]/[N_2] \approx 0.2$ and $R \approx 0.5$ and reaction (1) is 80% of reaction (3.18).

Fifty-two per cent of the O^+ ions are produced in metastable states. Of this 37% are $O^+(^2P)$ ions. If we assume that $O^+(^2P)$ behaves like $O^+(^2D)$, then 85% of all the O^+ ions produced will be converted into O_2^+ ions in the *E*-region. The remainder will charge exchange with N_2 to form N_2^+. This value (85%) takes into account that ~30% of the reactions of $O^+(^2D)$ with N_2 proceed via quenching as was shown by TORR and ORSINI (1978).

3.5 *Chemistry of* N_2^+

In the quiet daytime ionosphere N_2 is ionized primarily by absorption of ultraviolet photons:

$$N_2 + h\nu \rightarrow N_2^+ + e, \qquad (3.28)$$

by impact of energetic photoelectrons:

$$N_2 + e \rightarrow N_2^+ + e + e, \qquad (3.29)$$

and by charge transfer reactions with metastable O^+ ions:

$$O^+(^2D) + N_2 \xrightarrow{k_{12}} N_2^+ + O, \qquad (3.30)$$

$$O^+(^2P) + N_2 \xrightarrow{k_{13}} N_2^+ + O. \qquad (3.31)$$

The N_2^+ ions are removed primarily by reactions with atomic and molecular oxygen:

$$N_2^+ + O \xrightarrow{k_4} NO^+ + N, \qquad (3.32)$$

$$\xrightarrow{k_{14}} O^+ + N_2, \qquad (3.33)$$

$$N_2^+ + O_2 \xrightarrow{k_{15}} N_2 + O_2^+. \qquad (3.34)$$

[3.34 is insignificant at altitudes above ~150 km. The branching ratio for 3.33 is 7% (LINDINGER *et al.*, 1974)], and by dissociative recombination with electrons:

$$N_2^+ + e \xrightarrow{\alpha_3} N + N. \quad (3.35)$$

The chemistry of N_2^+ has proved to be considerably more complex than depicted by the above photochemistry. A quantitative study requires reliable values for the metastable O^+ densities. In the case of $O^+(^2P)$, measured values were obtained on AE from the VAE 7320 Å surface brightness observations. The sources and sinks of $O^+(^2P)$ have been quantitatively determined by WALKER *et al.* (1975), and RUSCH *et al.* (1977a). The situation regarding the concentration of $O^+(^2D)$ ions is not as simple. No measurements were made of this species on AE. It is therefore treated as an integral part of the photochemistry of N_2^+ and studied simultaneously with other processes which control the behavior of N_2^+ in the thermosphere. The chemistry of $O^+(^2P)$, on the other hand, is treated independently.

Prior to AE it was known that $O^+(^2D)$ is produced by photoionization and by photoelectron impact ionization of atomic oxygen. HENRY *et al.* (1969) determined the loss rate by electron quenching. GARSTANG (1956) calculated the radiative lifetime, and found it to be long (3.6 h). Laboratory measurements of RUTHERFORD and VROOM (1971) and STEBBINGS *et al.* (1966) indicated the $O^+(^2D)$ charge exchanges rapidly with N_2, i.e. at a gas kinetic rate. Prior to AE no information was available on rates at which $O^+(^2D)$ is quenched by O, O_2 and N_2. In addition to production by ionization of O, $O^+(^2D)$ ions are created by processes which deactivate $O^+(^2P)$. The photochemistry of $O^+(^2D)$ therefore comprises the following reactions:

Production:

$$O + h\nu \longrightarrow O^+(^2D) + e, \quad (3.36)$$

$$O + e \longrightarrow O^+(^2D) + 2e, \quad (3.37)$$

$$O^+(^2P) \longrightarrow O^+(^2D) + h\nu, \quad (3.38)$$

$$O^+(^2P) + e \xrightarrow{k_{17}} O^+(^2D) + e, \quad (3.39)$$

$$O^+(^2P) + O \xrightarrow{k_{18}} O^+(^2D) + O, \quad (3.40)$$

$$O^+(^2P) + N_2 \xrightarrow{k_{19}} O^+(^2D) + N_2. \quad (3.41)$$

Loss:

$$O^+(^2D) + N_2 \xrightarrow{k_{12}} N_2^+ + O, \quad (3.42)$$

$$O^+(^2D) + N_2 \xrightarrow{k_{20}} O^+(^4S) + N_2, \quad (3.43)$$

$$O^+(^2D) + O \xrightarrow{k_{21}} O^+(^4S) + O, \quad (3.44)$$

$$O^+(^2D) + e \xrightarrow{k_{22}} O^+(^4S) + e, \quad (3.45)$$

$$O^+(^2D) + O_2 \xrightarrow{k_{23}} O_2^+ + O. \quad (3.46)$$

[In previous studies (ORSINI *et al.*, 1977a, b; TORR and ORSINI, 1977) (3.43) was neglected, because laboratory measurements (RUTHERFORD and VROOM, 1971) indicated that k_{12} lay close to the Langevin limit. The present work which shows that (3.43) is not negligible updates all earlier work.]

The concentration of $O^+(^2P)$ is given by

$$\frac{1.15 J_1[O]}{0.218 + k_0[O] + k_{N_2}[N_2] + k_{N_e}[N_e]}, \quad (3.47)$$

where J_1 is the attenuated photoionization frequency. The factor of 1.15 includes the component due to photoelectrons discussed in Section 2.2; $k_0 = 5.2 \pm 2.5 \times 10^{-11}$ cm^3 s^{-1} (RUSCH *et al.*, 1977a), $k_{N_2} = 4.8 \pm 1.4 \times 10^{-10}$ cm^3 s^{-1} (RUSCH *et al.*, 1977a) and $k_{N_e} = 1.9 \times 10^{-7}(T_e/300)^{-0.5}$ cm^3 s^{-1} (HENRY *et al.*, 1969). A similar expression can be written for $[O^+(^2D)]$, i.e.

$$[O^+(^2D)] = \frac{Q_2}{k_{12}[N_2] + k_{20}[N_2] + k_{21}[O] + k_{22}[N_e] + k_{23}[O_2]}, \quad (3.48)$$

where Q_2 is the source of $O^+(^2D)$ due to photoionization, photoelectron impact excitation and deactivation of $O^+(^2P)$. We arrive at the following expression for $[N_2^+]$:

$$[N_2^+] = \frac{Q_1 + k_{12}[N_2][O^+(^2D)]}{k_4[O] + \alpha[N_e]}, \quad (3.49)$$

where Q_1 is the source of N_2^+ due to photoionization, photoelectron impact and charge exchange of $O^+(^2P)$ with N_2. Equations (3.48) and (3.49) may be combined to yield an expression which illustrates how the above chemistry can be used to readily determine all the rate coefficients shown in (3.48) and (3.49) from the AE data.

At low altitudes (200 km) (3.49) very nearly becomes $[N_2^+] = Q_1/k_4[O]$. Q_1 can be reliably calculated from AE data and k_4 is determined. This was done by D. TORR *et al.* (1977) and D. TORR (1979). D. TORR (1979) took into account recombination, and N_2 quenching of $O^+(^2D)$. Figure 13 shows a comparison of his results with those of MCFARLAND *et al.* (1974). The small discrepancy which occurred in the case of the earlier determination is removed.

Substituting for $O^+(^2D)$ in (3.49) we derive the equation

$$k_{12}[N_2] + k_{20}[N_2] + k_{21}[O] + k_{22}[N_e] + k_{23}[O_2] = k_{12}[N_2]R, \quad (3.50)$$

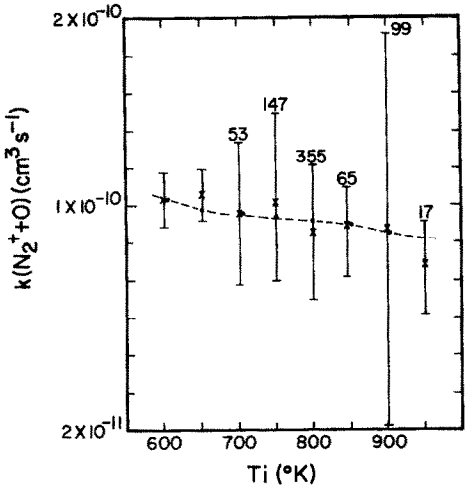

Fig. 13. The rate coefficient for the reaction $N_2^+ + O$ as a function of ion temperature. The broken curve is the laboratory results of McFarland *et al.* (1974). The crosses are the AE results of D. Torr (1978).

where

$$R = \frac{Q_2}{(k_4[O] + \alpha_3 N_e) - Q_1}, \qquad (3.51)$$

i.e. R is the ratio of the total $O^+(^2D)$ production to loss by charge exchange, and is calculated from the AE measurements. Equation (3.50) simply states that the $O^+(^2D)$ loss frequency is equal to the $O^+(^2D)$ production frequency. It is formulated to illustrate the ease with which all the rate coefficients can be unambiguously determined. For example if we select data where $\alpha_3 N_e \ll k_4[O]$ we remove the effects of uncertainties in α_3 from R. If the altitude range is limited to heights greater than 220 km, $k_{23}[O_2]$ is negligible. Rearranging (3.50) under these conditions we find

$$k_{21} - k_{20}\frac{[N_2]}{[O]} = k_{12}\frac{[N_2]}{[O]}(R-1) - k_{22}\frac{[N_e]}{[O]}. \qquad (3.52)$$

All the terms on the right-hand side are known, with the exception of k_{12} which has only been measured at energies greater than 0.5 eV (Rutherford and Vroom, 1971). Figure 14 shows the results of plotting $[N_2]/[O]$ against the right-hand side of (3.52) for several values of k_{12}. The results show that $k_{21} \approx 0 (\ll 3 \times 10^{-11}\ \mathrm{cm^3\ s^{-1}})$. Therefore the term $k_{21}[O]$ can be dropped from (3.50). Rearranging (3.52) to solve for k_{12} and k_{20} we obtain

$$k_{20} + k_{12}(1-R) = k_{22}\frac{[N_e]}{[N_2]}. \qquad (3.53)$$

The results of plotting $1-R$ against $k_{22}[N_e]/[N_2]$ are shown in Fig. 15a. These results show

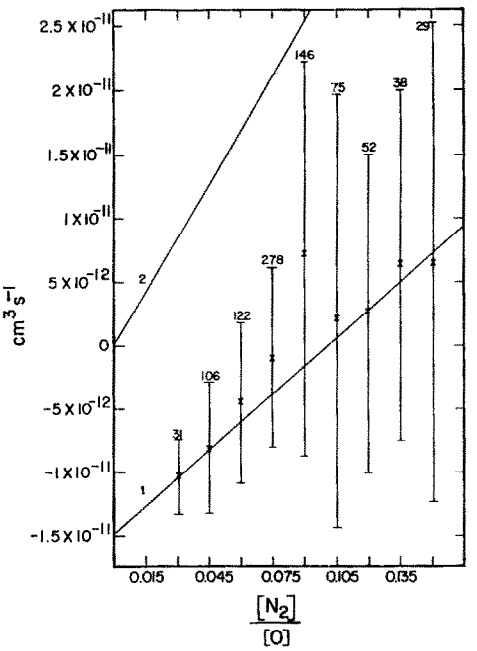

Fig. 14. The ratio $[N_2]/[O]$ plotted against the right-hand side of (3.52). The slope gives k_{20} (N_2 quenching of $O^+(^2D)$) and the intercept k_{21} (O quenching). A value of $1 \times 10^{-10}\ \mathrm{cm^3\ s^{-1}}$ was used for k_{12} (charge exchange) for curve (1) and $2.5 \times 10^{-10}\ \mathrm{cm^3\ s^{-1}}$ for curve 2. The results imply that $k_{21} \approx 0$.

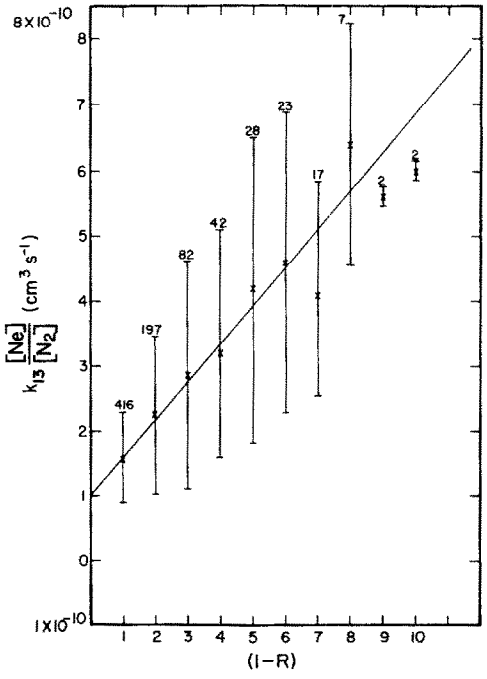

Fig. 15a. The ratio $[N_e]/[N_2]$ as a function of the quantity $(1-R)$ in (3.53). The slope gives k_{12} (charge exchange) and the intercept k_{20} (N_2 quenching); here $k_{21} = 0$.

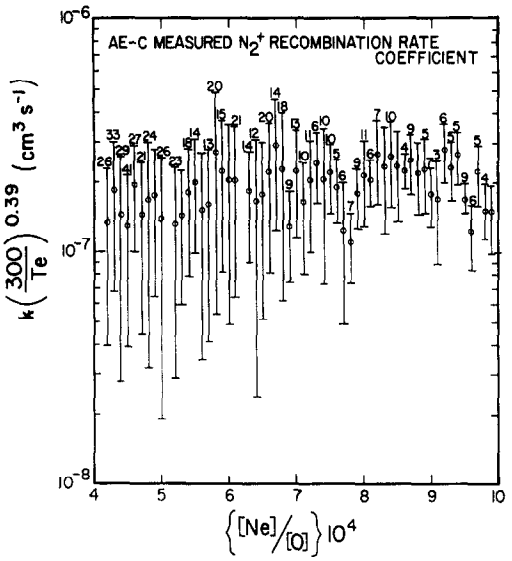

Fig. 15b. The recombination rate coefficient of N_2^+ determined from AE data as a function of $[N_e]/[O]$.

that $k_{20} < 2\times10^{-10}\,cm^3\,s^{-1}$ and that $k_{12} = 1\begin{Bmatrix}+1\\-0.5\end{Bmatrix}\times10^{-10}\,cm^3\,s^{-1}$. Thus we conclude that charge exchange of $O^+(^2D)$ with N_2 is about an order of magnitude smaller at thermal energies than at $E > 0.5$ eV (cf. RUTHERFORD and VROOM, 1971). N_2 quenching accounts for about 30% of all the reactions of $O^+(^2D)$ with N_2.

Using the above chemistry N. ORSINI has independently determined the N_2^+ recombination rate coefficient, α_3 including reaction (3.43). His unpublished results are shown in Fig. 15b. The agreement with the laboratory results of MEHR and BIONDI (1969) is good. This updates the earlier result published by ORSINI *et al.* (1977b).

3.6 *Diurnal variations of ion concentrations*

In the preceeding sections we have described how the AE data were used in special studies designed to isolate specific processes to determine

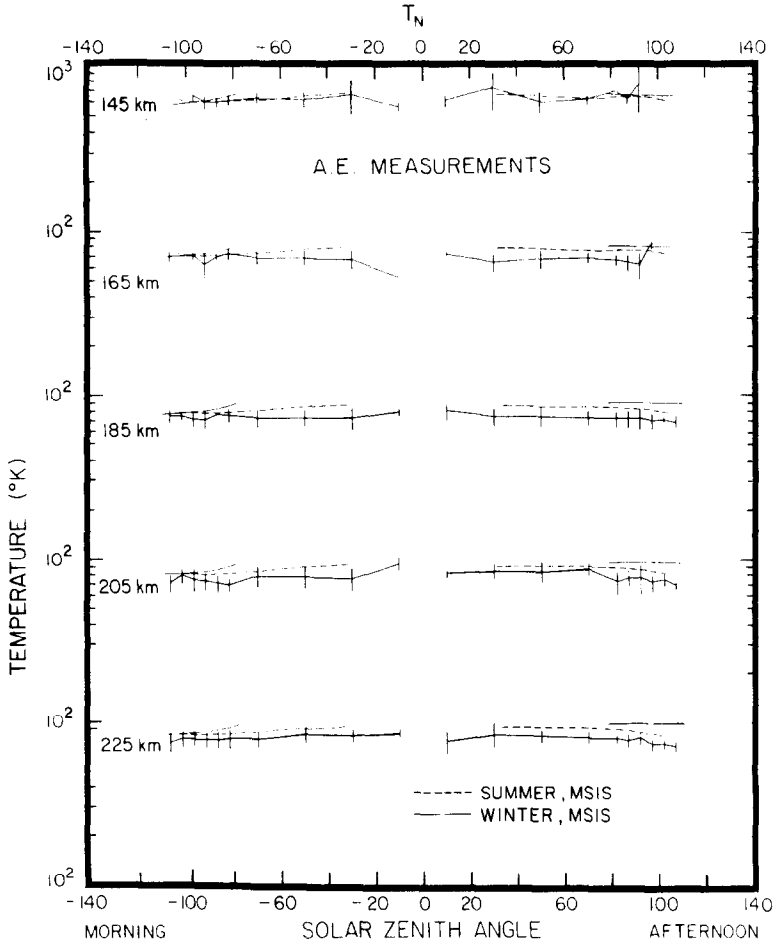

Fig. 16. The measured neutral temperature (SPENCER *et al.*, 1973) as a function of solar zenith angle and altitude averaged for the period 1974–76 from D. TORR *et al.* (1979).

or confirm the relevant rate coefficients. The combined information emerging from these studies has brought us to a point where it is possible to develop a model of the photochemical regime of the *F1*-layer, sufficiently free of ambiguity to provide a valid check on the overall photochemical picture of the major constituents in this region. Such a study was carried out by D. TORR *et al.* (1979). The purpose of the study was to check the overall consistency of the photochemistry. They excluded those regimes from the study where transport effects or ionization by sources such as precipitating particles are significant, i.e. they used altitudes below 220 km, solar zenith angles less than ~100° and invariant latitudes less than 55°. This corresponds to the sunlit *F1*-layer of the mid-latitude ionosphere.

Several theoretical models have been described in the literature which attempt to describe the diurnal variation of the *F1*-layer (see for example, KENESHEA *et al.*, 1970; TORR *et al.*, 1972; SCHUNK and WALKER, 1973). Until now we have not had direct measurements of ion concentrations made over a full diurnal cycle with which to compare such models. This situation has been remedied with the AE database. D. TORR *et al.* (1979) used almost all the data taken by AE-C to determine as a function of altitude the diurnal, seasonal and latitudinal variation of ion concentrations, and the input parameters required to model the former. They found that data taken below 225 km could be averaged as a function of altitude and solar zenith angle. Use of the latter parameter eliminates nearly all of the seasonal and latitudinal variations. Averages of directly measured quantities such as $[O^+]$, $[NO^+]$, $[O_2^+]$, $[N_2^+]$, $[O]$, $[N_2]$, T_n, T_i, and T_e were calculated together with standard deviations at intervals of 10 km in altitude and 10° in solar zenith angle.

Average maps for T_n, T_i and T_e are shown in Figs. 16–18, respectively. The approximate number of samples per bin is several hundred. Figures 19

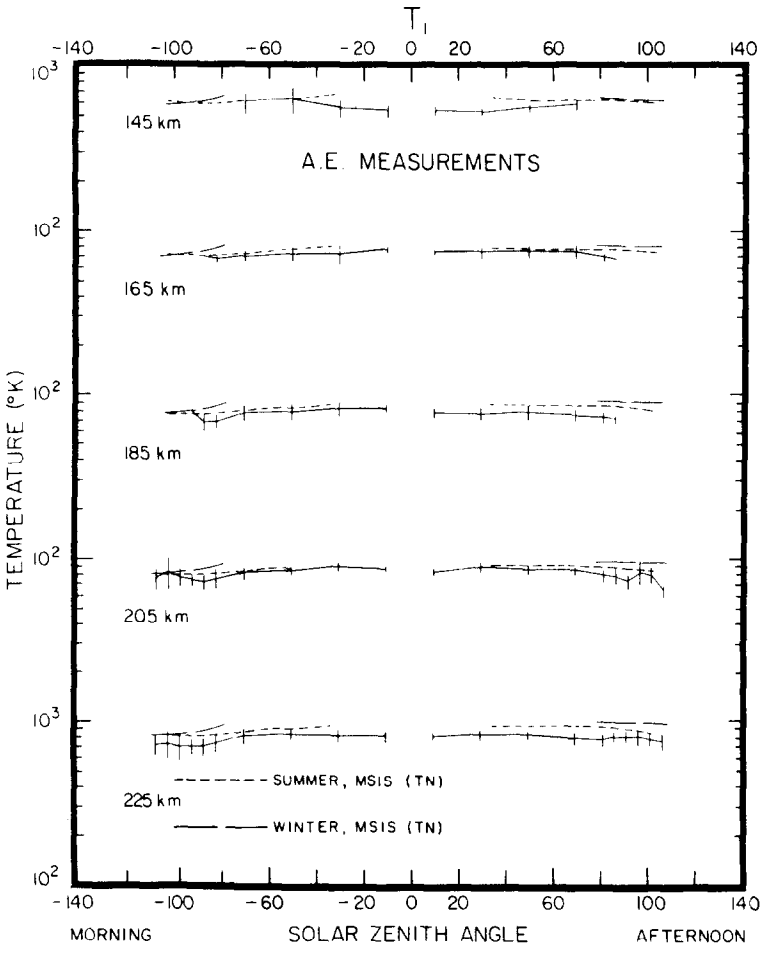

Fig. 17. Same as Fig. 16 for T_i (HANSON *et al.*, 1973) (cf. D. TORR *et al.*, 1979).

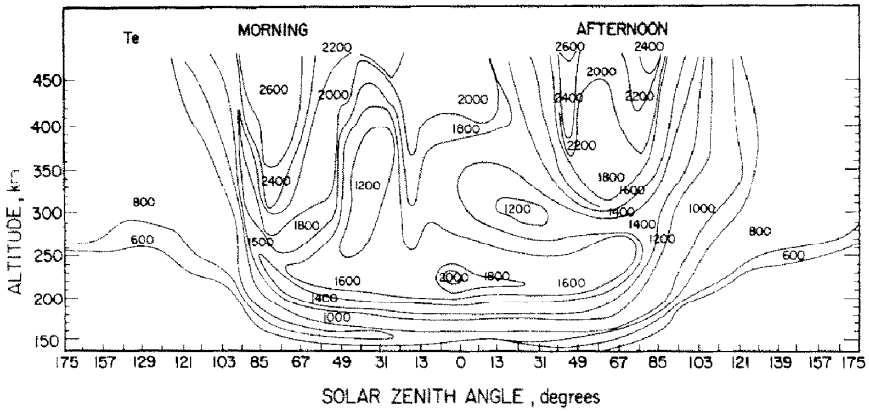

Fig. 18. Contours of constant T_e as a function of altitude and solar zenith angle derived from AE-C measurements (BRACE *et al.*, 1973) (D. TORR *et al.*, 1979).

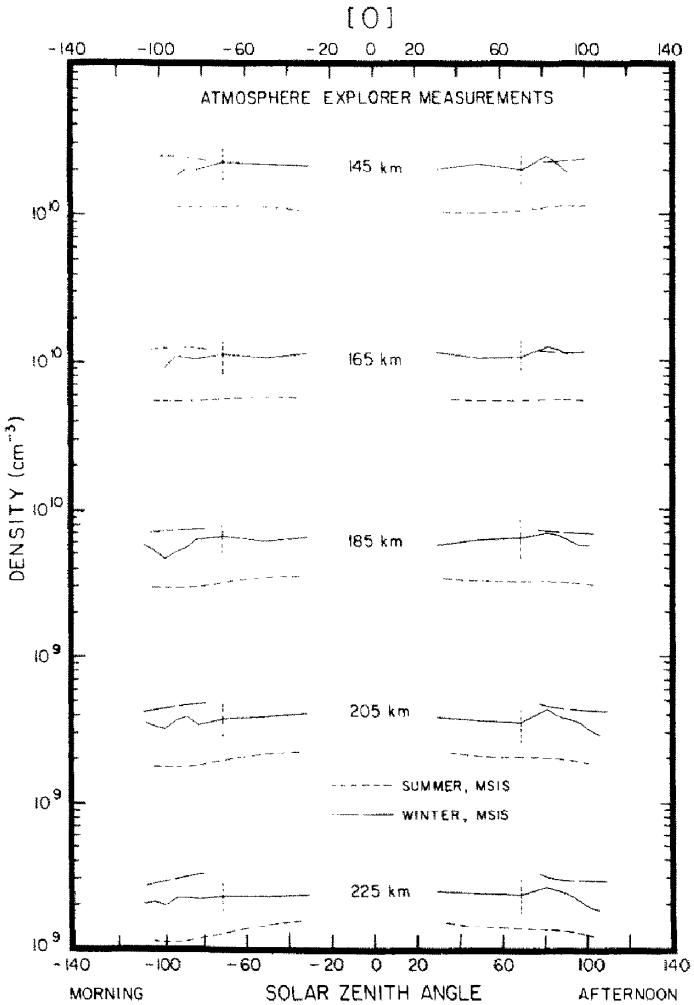

Fig. 19. Same as Fig. 16 for [O] (PELZ *et al.*, 1973; NIER *et al.*, 1973) (cf. D. TORR *et al.*, 1979).

and 20 show the diurnal variations of [O] and [N_2]. Values for the O_2 density were determined from both the O_2^+ ion chemistry discussed in Section 3.4 (cf. OPPENHEIMER *et al.*, 1976) and from direct measurements of [O_2]. Only a limited sample of directly measured values of [O_2] were available because the quantity measured by conventional neutral mass spectrometers is the total oxygen abundance 2[O_2]+[O] which is not easily resolved into atomic and molecular components. NIER *et al.* (1974) developed a new technique to measure the [O_2] in which use is made of the satellite velocity to distinguish atmospheric [O_2] from [O_2] which is formed by the recombination of atomic oxygen on the walls of the instrument. D. TORR *et al.* (1979) also attempted to use the method described by KIRBY-DOCKEN and OPPENHEIMER (1977). The method involves subtracting extrapolated [O] from the total oxygen concentration. D. TORR *et al.* found, however, then even at altitudes as low as 150 km the [O_2] comprised such a small fraction of the total oxygen abundance that the subtraction of the atomic oxygen component extrapolated from higher altitudes (assuming diffusive equilibrium) resulted in large errors. This method was therefore not used in deriving the O_2 densities which are given in Fig. 21.

Ion concentrations were calculated by D. TORR *et al.* (1979) using the chemistry and rate coefficients described in the preceeding sections. Figures 22–26 show the measured and theoretical ion concentrations as a function of zenith angle. In general the agreement between experiment and theory is very good. In the case of [O^+] and [N_2^+] there is

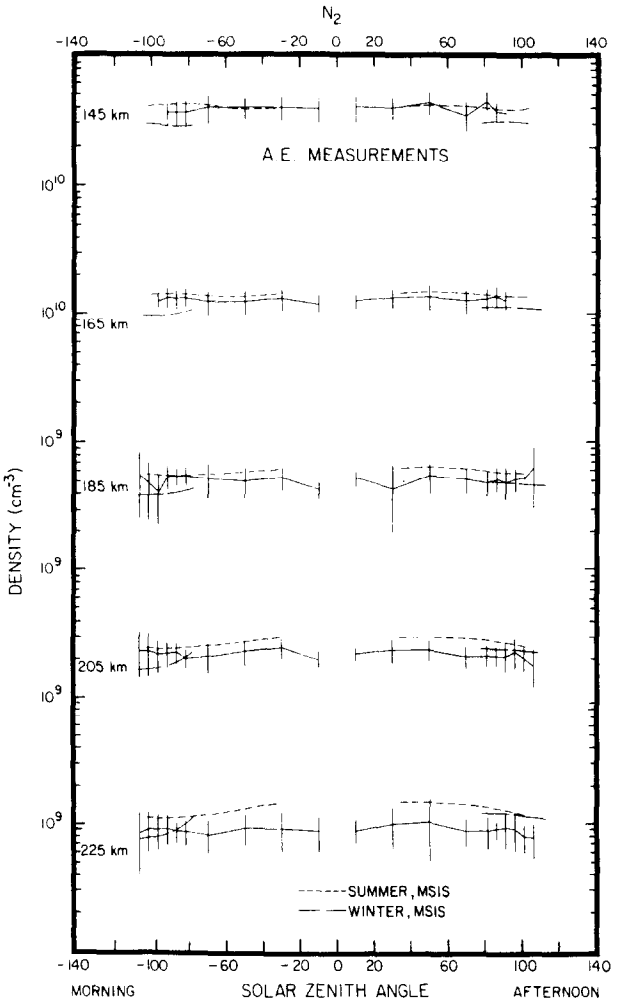

Fig. 20. Same as Fig. 19 for N_2.

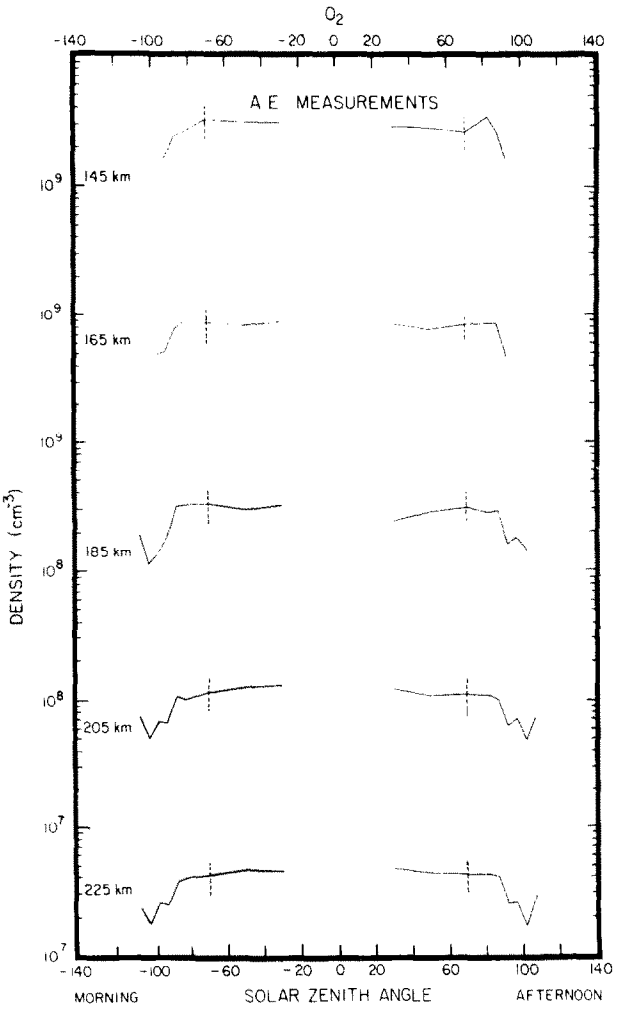

Fig. 21. The average concentration of O_2 derived as a function of zenith and altitude from both direct measurements of $[O_2]$ at ~200 km by OSS (NIER *et al.*, 1973, 1974) and from the O^+ ion chemistry using measured parameters (D. TORR *et al.*, 1979).

some disagreement at 145 km. This is due to the 'ram effect'. The latter is not well understood, but is seen as an increase in low ion concentrations ($<10^3$ cm^3) when the ion mass spectrometer is looking into the satellite velocity vector at low perigree altitudes (<150 km). The fact that the O_2^+ and NO^+ concentrations agree well with the measured values establishes the validity of the theoretical values for the low altitude $[O^+]$ and $[N_2^+]$ since O_2^+ is produced mainly by the reaction $O^+ + O_2 \rightarrow O_2^+ + O$ and N_2^+ by $N_2^+ + O \rightarrow NO^+ + N$.

3.7 *Ion chemistry conclusion*

These results show that with the parameters measured by the AE satellite it has been possible to reduce ambiguities and uncertainties in the photochemistry of the major species of the daytime, mid-latitude *F*-layer to the point where we now believe that this photochemistry is well determined. There is no longer any leeway to scale rate coefficients and branching ratios by factors of 2 or more, as has been done in the past in order to bring theory into agreement with measurement.

Table 3 summarizes all rate coefficients used in Section 3.

4. THERMOSPHERIC CHEMISTRY

4.1 *Introduction*

This section of the review deals primarily with results of neutral metastable species measured by

Table 3. Ionospheric rate coefficients

Reaction	Rate coefficients ($cm^3 s^{-1}$)	
$O^+ + N_2 \xrightarrow{k_1} NO^+ + N$	$k_1 = k_3$ see equation (3.15)	St-Maurice and Torr (1978); Albritton *et al.* (1977)
$NO^+ + e \xrightarrow{\alpha_1} N + O$	$4.2\times10^{-7}(T_e/300)^{-0.85}$	M. Torr and Torr (1979a); Walls and Dunn (1974)
$N(^2D) + O \xrightarrow{k_{2a}} NO^+ + e - 0.37\,eV$	$k_{2a} \lesssim 2\times10^{-13}$ for $T_{eff} < 1000\,K$	M. Torr and Torr (1979b)
$N_2^+ + O \xrightarrow{k_4} NO^+ + N$	$1.4\times10^{-10}(T_i/300)^{-0.44} T < 1500\,K$	D. Torr *et al.* (1977); D. Torr (1979); McFarland *et al.* (1974)
$N_2^+ + O \longrightarrow O^+ + N_2$	$0.07\,k_4(T/300)^{0.21}$	McFarland *et al.* (1974)
$N^+ + O_2 \xrightarrow{k_5} NO^+ + O$	2×10^{-10}	Huntress and Anicich (1976)
$N^+ + O_2 \longrightarrow O_2^+ + N$	4×10^{-10}	Huntress and Anicich (1976)
$N^+ + O_2 \longrightarrow O^+ + NO$	2×10^{-11}	Huntress and Anicich (1976)
$O_2^- + N \xrightarrow{k_6} NO^+ + O$	1.8×10^{-10}	Goldan *et al.* (1966)
	1.0×10^{-10}	D. Torr *et al.* (1976d)
$O_2^+ - NO \xrightarrow{k_7} NO^+ + O_2$	4.4×10^{-10}	Lindinger *et al.* (1975)
$O_2^+ + e \xrightarrow{\alpha_2} O + O$	$1.6\times10^{-7}(T_e/300)^{-0.55}$	D. Torr *et al.* (1076c); Mehr and Biondi (1969)
$O^+ + O_2 \xrightarrow{k_8} O_2^+ + O$	see equation (3.21)	St-Maurice and Torr (1978); Albritton *et al.* (1977)
$O^+(^2D) + O_2 \xrightarrow{k_9} O_2^+ + O$	$k_9 = k_{23} = 1 \pm 0.6\times10^{-10}$	D. Torr *et al.* (1978)
$N_2^+ + e \xrightarrow{\alpha_3} N + N$	$1.8\times10^{-7}(T_e/300)^{-0.39}$	Mehr and Biondi (1969): confirmed by N. Orsini (unpublished) (see Fig. 15b)
$O^+(^2D) + N_2 \xrightarrow{k_{12}} N_2^+ + O$	$1\begin{Bmatrix}+1\\-0.5\end{Bmatrix}\times10^{-10}$	D. Torr and Orsini (1978); this paper Fig. 15a.
$O^+(^2P) + N_2 \xrightarrow{k_{13}} N_2^+ + O$	$4.8 \pm 1.4\times10^{-10}$	Rusch *et al.* (1977a)
$N_2^- + O_2 \xrightarrow{k_{15}} O_2^+ + N_2$	$\sim 1.5\times10^{-11}$ at 800 K see reference for T dependence	Lindinger *et al.* (1974)
$O^+(^2P) + e \xrightarrow{k_{17}} O^+(^2D) + e$	$1.5\times10^{-7}\,(300/T_e)^{1/2}$	Henry *et al.* (1969)
$O^+(^2P) + O \xrightarrow{k_{18}} O^+ + O$	$5.2 \pm 2.5\times10^{-10}$	Rusch *et al.* (1977a)
$O^+(^2P) + N_2 \xrightarrow{k_{19}} O^+(^2D) + N_2$	assumed $k_{19} = 0$	
$O^+(^2D) + N_2 \xrightarrow{k_{20}} O^+(^4S) + N_2$	$2\times10^{-11} < k_{20} < 2\times10^{-10}$	(This paper)
$O^+(^2D) + O \xrightarrow{k_{21}} O^+(^4S) + O$	$<1\times10^{-11}$	Orsini *et al.* (1977); (this paper Fig. 14)
$O^+(^2D) + e \xrightarrow{k_{22}} O^+(^4S) + e$	$7.8\times10^{-8}(T_e/300)^{1/2}$	Henry *et al.* (1969)

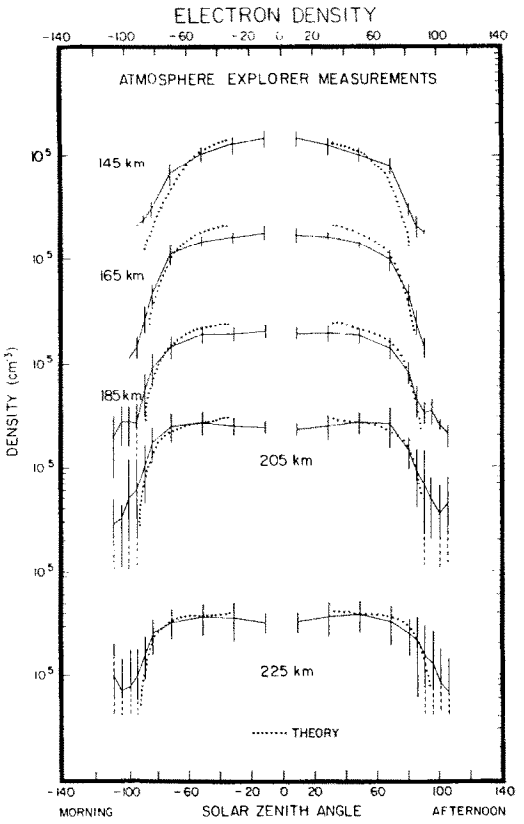

Fig. 22. Average measured and calculated electron densities as a function of solar zenith angle and altitude. Data used were taken over the period 1974–76 (D. TORR *et al.*, 1979).

the visible airglow experiment (VAE) (HAYS *et al.*, 1973), and odd nitrogen concentrations measured by the UV nitric-oxide experiment (BARTH *et al.*, 1973), and the open source neutral mass spectrometer (NIER *et al.*, 1973). Although the substance of the AE work done in this area is comparable in extent to that in ion chemistry we have kept this section brief, because it is not possible within the scope of this treatment to cover all aspects of the AE work on ionospheric and thermospheric chemistry. Highlights that we discuss include odd nitrogen measurements and theory, including diurnal, seasonal and latitudinal variations; sources and sinks of $O(^1S)$ and $O(^1D)$ atoms including the diurnal variation of the latter; the section is concluded with a study of the source of $N_2[2P](0\text{–}0)$ emission in the thermosphere.

4.2 *Atomic nitrogen*

One of the first results to emerge from the analyses of the AE data were deductions by RUSCH *et al.* (1975a) that the peak concentrations of $N(^4S)$ must exceed $\sim 10^7$ cm^{-3}. This conclusion was based on an analysis of 5200 Å airglow measurements by VAE. The 5200 Å emission arises from the transition $N(^4S\text{–}^2D)$ and is a direct measure of the ^2D density. Surface brightness measurements were inverted to yield volume emissions rate profiles as a function of altitude. Thus, sources and sinks of $N(^2D)$ could be studied as a function of altitude. Prior to AE, details of the chemistry of $N(^4S)$ and $N(^2D)$ were uncertain. The satellite studies resulted in a large reduction in these uncertainties.

Figure 27 summarizes the processes which result in the production and destruction of nitrogen atoms in the thermosphere. Atomic nitrogen is produced primarily by ion–atom interchange of N_2^+ with O

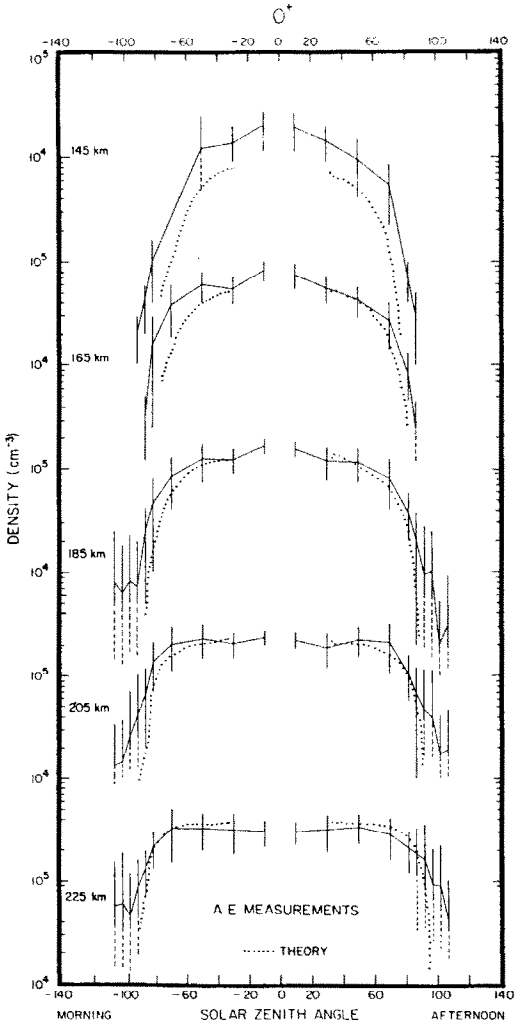

Fig. 23. Same as Fig. 22 for $[O^+]$.

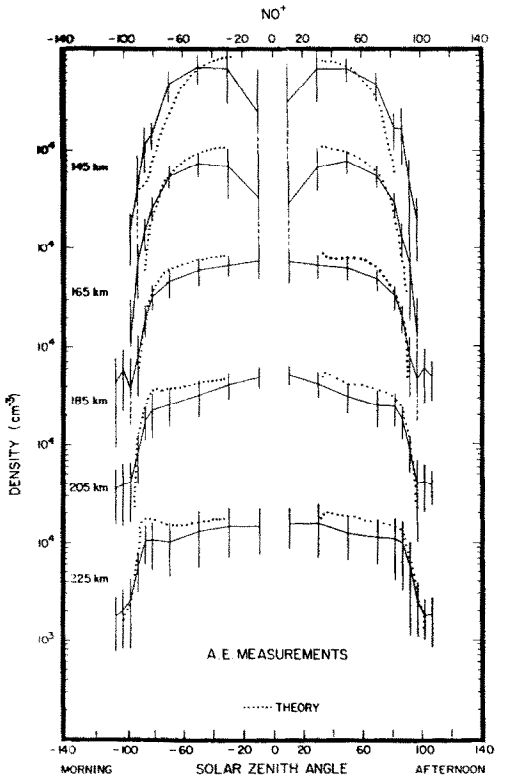

Fig. 24. Same as Fig. 22 for $[NO^+]$.

and by dissociative recombination of NO^+ at altitudes above 200 km. Above 300 km recombination of N_2^+ becomes a significant source. Below 200 km photoelectron impact dissociation of N_2 dominates. The branching ratios for the production of $N(^2D)$ and $N(^4S)$ are critical in determining the NO and $N(^4S)$ densities in the thermosphere, because $N(^2D)$ produces NO and the odd nitrogen is cannibalistically destroyed. Predominant production of $N(^2D)$ at low altitudes results in an NO rich atmosphere, since $N(^2D)$ reacts with O_2 to form NO. The latter in turn destroys $N(^4S)$. The ratio of $[O]/[O_2]$ increases with altitude and O quenching of $N(^2D)$ becomes the main source of $N(^4S)$. The latter in turn becomes a major source of NO by reacting with O_2, a reaction which is highly temperature dependent. The buildup of $N(^4S)$ tends to be self sustaining.

Studies by Norton and Barth (1970), Strobel *et al.* (1970), and Rusch (1973) identified the following production and loss mechanisms.

4.2.1 $N(^2D)$. $N(^2D)$ is produced mainly by the processes:

$$NO^+ + e \xrightarrow{\beta_1\alpha_1} N(^2D) + O, \quad (4.1)$$

$$N_2^+ + e \xrightarrow{2\beta_2\alpha_3} N(^2D) + N, \quad (4.2)$$

$$N_2^+ + O \xrightarrow{\beta_3 k_4} N(^2D) + NO^+, \quad (4.3)$$

$$e + N_2 \xrightarrow{\beta_4 J_4} N(^2D) + N, \quad (4.4)$$

$$N^+ + O_2 \xrightarrow{k_{24}} N(^2D) + O_2^+. \quad (4.5)$$

The loss processes are:

$$N(^2D) + O \xrightarrow{k_{2b}} N(^4S) + O, \quad (4.6)$$

$$N(^2D) + O_2 \xrightarrow{k_{25}} NO + O. \quad (4.7)$$

$$N(^2D) + e \xrightarrow{k_{26}} N(^4S) + e. \quad (4.8)$$

In addition to (4.6) Zipf (1978) has observed that energetic $N(^2D)$ atoms associatively ionize in the laboratory to form NO^+, i.e.

$$N(^2D) + O(^3P) \xrightarrow{k_{2a}} NO^+ + e - 0.37\,\text{eV}. \quad (4.9)$$

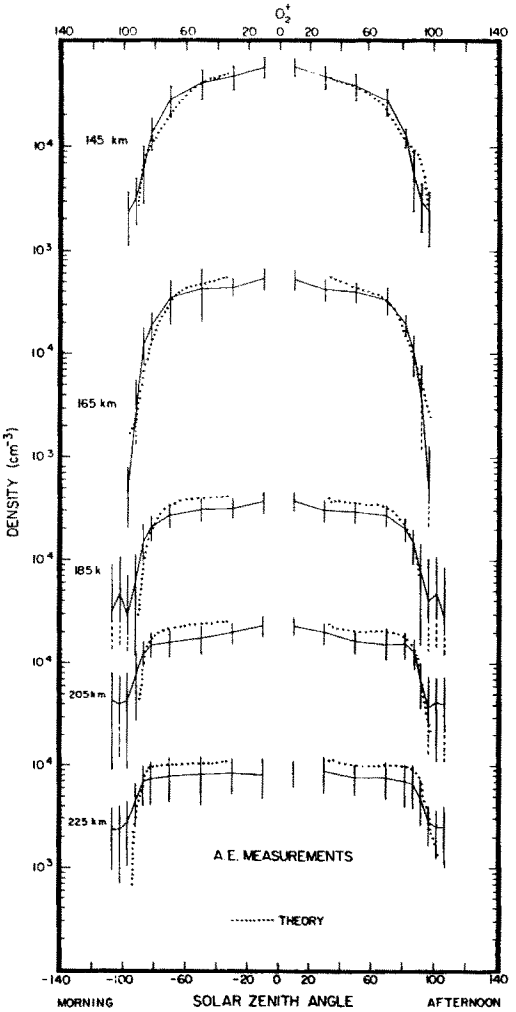

Fig. 25. Same as Fig. 22 for $[O_2^+]$.

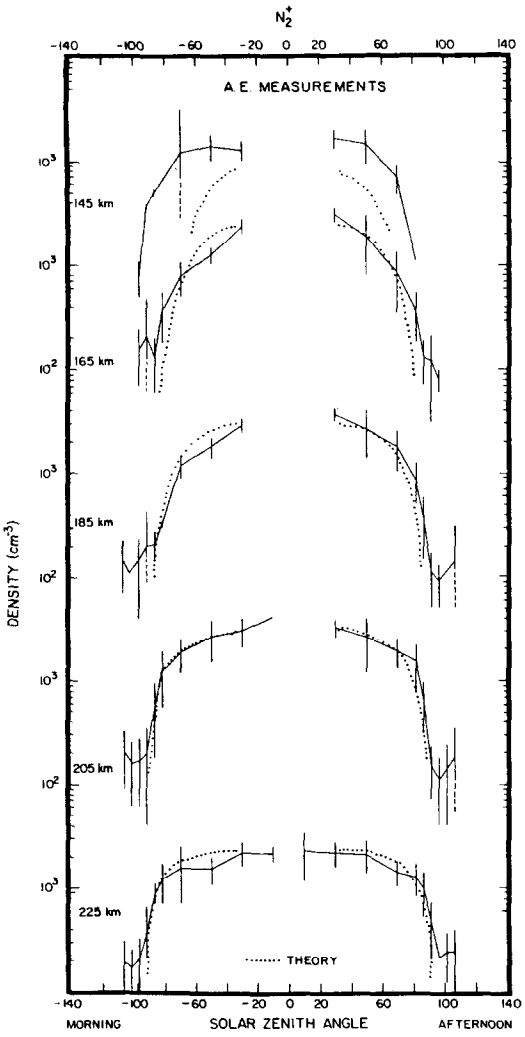

Fig. 26. Same as Fig. 22 for $[N_2^+]$.

Reaction (4.9) has also been investigated using AE data to establish whether it is a significant sink for $N(^2D)$ atoms at thermal temperatures (M TORR and TORR, 1979b)

Prior to AE the branching ratios β_1 to β_4, the rate coefficients k_{2b}, k_{25} and k_{26} were unknown or uncertain. Values deduced for β_1 from early photochemical studies (HERNANDEZ and TURTLE, 1969; STROBEL *et al.*, 1970; NORTON and BARTH, 1970; ORAN *et al.*, 1975) ranged from 0.1 to 0.85. From theoretical studies BARDSLEY (1968) estimated $0.5 \leq \beta_1 \leq 1$. In the case of k_{25}, three laboratory measurements had been made, with two in close agreement giving $k_{25} \approx 6 \times 10^{-12}$ cm^3 s^{-1} (BLACK *et al.*, 1969; LIN and KAUFMAN, 1971). The third measurement gave $k_{25} = 4.4 \times 10^{-12}$ (SLANGER *et al.*, 1971). In the case of k_{26}, HENRY and WILLIAMS (1968) and SEATON (1956) calculated values of 3×10^{-9} cm^3 s^{-1} and 8.0×10^{-10} cm^3 s^{-1}, respectively.

Using the VAE 5200 Å data and the measured neutral ion densities and temperatures and photoelectron fluxes, RUSCH *et al.* (1975a) drew the following conclusions.

(1) The yield of $N(^2D)$ must be near the maximum allowable value, i.e. $\beta_1 \approx \beta_2 \approx \beta_3 \approx 1.0$.

(2) Quenching by atomic oxygen is a major loss process for $N(^2D)$ in the thermosphere; $k_{2b} \lesssim 6 \times 10^{-13}$ cm^3 s^{-1} which tends to agree with early ground based work of WEILL (1969).

(3) Electron quenching is important above 250 km.

(4) O_2 quenching is important below 200 km.

These conclusions were confirmed by subsequent aeronomic investigations by STROBEL *et al.* (1976) and FREDERICK and RUSCH (1977). The latter work narrowed down the uncertainties on these rate coefficients further.

The atomic oxygen quenching rate coefficient was subsequently measured in the laboratory by DAVENPORT *et al.* (1976). They derived a value of 2×10^{-12} cm^3 s^{-1} at 300 K which increases to $\sim 1 \times 10^{-11}$ cm^3 s^{-1} at 700 K if a conservative value of 0.5 kcal mole^{-1} is adopted for the activation energy for the reaction implied by the measurements. This directly contradicts the aeronomic determination of k_{2b}. It is conceivable that reaction (4.9) might explain part of the discrepancy between the aeronomic and laboratory results. However, this would require that the laboratory reactants possess sufficient translational energy to partially counteract the energy deficit.

A subsequent quantitative study using both nighttime and daytime AE data by FREDERICK and RUSCH (1977) reconfirmed the low value for k_{2b} (4×10^{-13} cm^3 s^{-1}). TORR and TORR 1979b) have deduced an upper limit of $\sim 2 \times 10^{-13}$ cm^3 s^{-1} for k_{2a} in the nighttime mid-latitude ionosphere. FREDERICK and RUSCH determined that the electron quenching rate of $N(^2D)$ lies between 3.6–$6.5 \times 10^{-10}(T_e/300)^{1/2}$ cm^3 s^{-1}. They found k_{25} (the O_2 quenching rate coefficient) to be in good agreement with the laboratory results, i.e. $6 \pm 1 \times 10^{-12}$ cm^3 s^{-1} (LIN and KAUFMAN, 1971). From combined laboratory and aeronomic studies ZIPF (1978) has estimated that the fractional yield of N^+, $N(^2P)$, $N(^2D)$ and $N(^4S)$ atoms from electron impact dissociation of N_2 is approximately 0.135: 0.155: 0.31: 0.40, respectively at 100 eV. Figures 28 and 29 show the production and loss rates of $N(^2D)$ calculated by FREDERICK and RUSCH (1977) for AE-C orbit

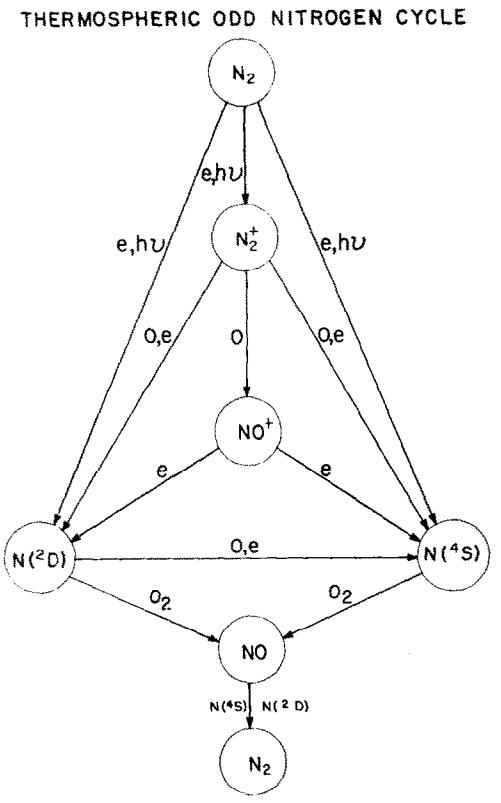

Fig. 27. Schematic illustration of the chemistry of $N(^2D)$, $N(^4S)$ and NO in the thermosphere.

1663 using the above rate coefficients. Figures 30 and 31 show a comparison of the theoretical 5200 Å results with VAE measurements for a nighttime and daytime orbit. These results illustrate the quality of the agreement between experiment and theory using the AE rate coefficients. The solid curve in Fig. 31 demonstrates that the high laboratory values for $k_{2b}[N(^2D)+O]$ are inconsistent with the satellite measurements.

4.2.2 $N(^4S)$. Because the chemistry of $N(^2D)$ demands that branching ratios for the production of $N(^2D)$ must be high, the only important sources of $N(^4S)$ are (4.6) (O quenching of $N(^2D)$) and (4.4) (photoelectron impact dissociation of N_2). There are several other minor sources of $N(^4S)$ which are shown in Fig. 32 from Rusch *et al.* (1977b). This figure illustrates the crucial role played by atomic oxygen quenching of $N(^2D)$ in the chemistry of $N(^4S)$. At auroral altitudes the branching ratio for the production of $N(^4S)$ and $N(^2D)$ by electron impact is the most critical parameter determining the ratio $[N(^4S)]/[NO]$.

4.2.3 $N(^4S)$ *loss rates.* $N(^4S)$ is lost mainly by the reactions

$$N(^4S)+O_2 \xrightarrow{k_{27}} NO+O, \qquad (4.10)$$

$$N(^4S)+NO \xrightarrow{k_{28}} N_2+O. \qquad (4.11)$$

The ratio of the O to O_2 densities is also a major factor determining the ratio of $N(^4S)$ to NO densities. Uncertainties in the O_2 density on AE is the primary source of uncertainty in odd nitrogen calculations.

4.2.4 *Nitric oxide.* Reactions (4.7) and (4.10) define the thermospheric sources of nitric oxide. Reaction (4.11) is the main sink for NO, although under certain conditions minor loss processes with

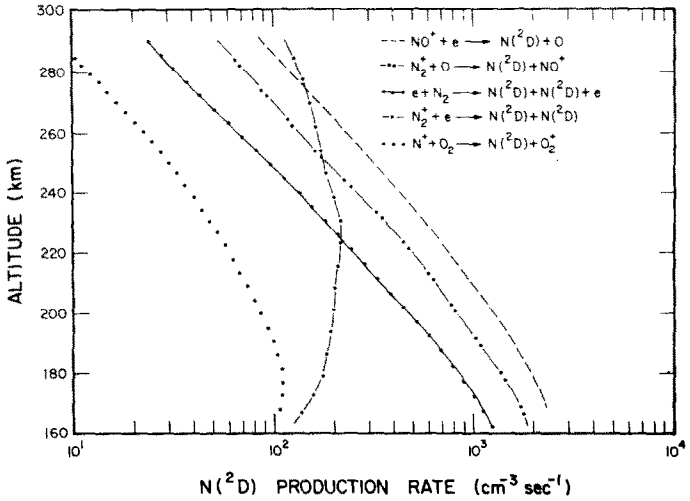

Fig. 28. The production rate of $N(^2D)$ for AE-C orbit 1663 downleg on 14 May 1974 (Frederick and Rusch, 1977).

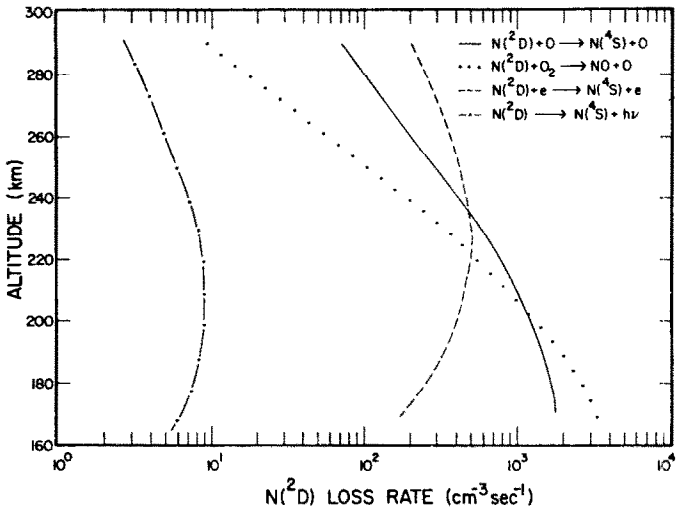

Fig. 29. N(^2D) loss rates for AE-C orbit 1663 downleg on 14 May 1974.

ions become important enough to influence the odd nitrogen chemistry.

At altitudes above 160 km the N(^4S) sinks become small due to the rapid decrease in O_2 and NO, and [N(^4S)] is controlled by diffusion. Diffusion becomes important in the case of NO at altitudes above 250 km. At low altitudes, N(^2D) is converted primarily into NO which cannibalistically destroys N(^4S) and causes it to peak at about 140 km. Therefore at low altitudes the NO diffusion lifetime is shorter than the chemical lifetime,

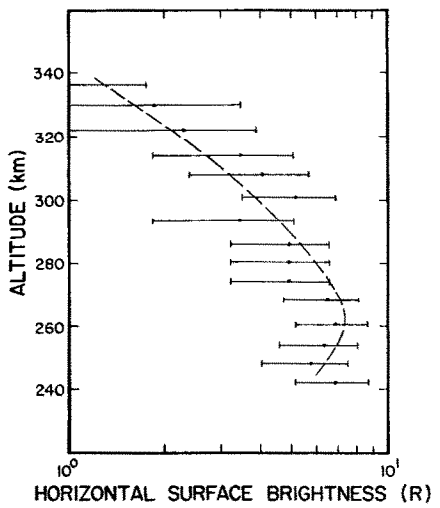

Fig. 30. Horizontally viewed surface brightness of the 5200 Å emission for AE-C nighttime orbit 3682 downleg (points). The broken curve is the theoretical results of FREDERICK and RUSCH (1977).

and transport of NO into the mesosphere becomes a major thermospheric removal process.

Taking these factors into account RUSCH *et al.* (1975a, 1977b) modeled the odd nitrogen concentrations in the thermosphere and arrived at the results shown in Fig. 33 for AE-C orbit 594.

4.2.5 *AE measurements of* N(^{4}S) *and* NO. The high N densities deduced from the airglow measurements were confirmed soon thereafter by direct measurements by MAUERSBERGER *et al.* (1975) using the open source neutral mass spectrometer (OSS). Atomic nitrogen had been detected by FELDMAN and TAKACS (1974) by using optical spectroscopy. They used the γ- and δ-emission bands of NO to derive N densities of $\sim 1.9 \times 10^7$ cm at 140 km. The atomic nitrogen appeared to be in diffusive equilibrium above this altitude. GHOSH *et al.* (1968) using a rocket-borne mass spectrometer had previously reported an abundance of N which could be as much as 6% of [N_2]. The AE results were further borne out by satellite measurements by GERARD (1975) who measured the NO δ-bands.

The neutral mass spectrometer measurements of MAUERSBERGER *et al.* (1975) were of special significance in that they identified the presence of a peak at mass 30 as being due primarily to N(^4S) which had recombined with oxygen present on the surface of the instrument to form NO. This technique has subsequently become a standard way of measuring the N(^4S) density. It can also be used at lower altitudes if the NO density is independently measured and subtracted from the total mass 30 measurement (ENGEBRETSON *et al.*, 1977a).

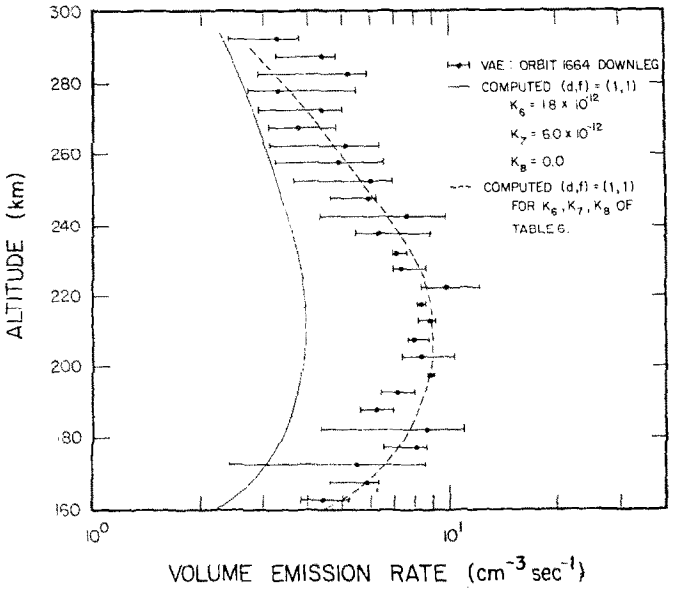

Fig. 31. Measured and calculated volume emission rate profiles for AE-C daytime orbit 1664 downleg. The broken curve was obtained by FREDERICK and RUSCH (1977) using the AE rate coefficients. The solid curve shows the effect of using 1.8×10^{-12} cm^3 s^{-1} for the rate coefficient for O quenching N(^2D).

MAUERSBERGER *et al.* (1975) observed a clear diurnal variation in both the mass 14 used and mass 30 peaks. They deduced a peak density of $\sim 10^6$ cm^{-3} at 400 km.

Figure 34 shows the diurnal variation of N(^4S) densities measured by the neutral atmosphere composition experiment (CARIGNAN and RUSCH, 1978) on AE-E. Also shown are their theoretical calculations which incorporated the chemistry described above. Uncertainties in the theoretical results arise primarily from uncertainties in the O_2 concentration.

The agreement or disagreement between experimental and theoretical results at this stage cannot be taken to be meaningful. The experimental technique of measuring N(^4S), while highly successful, has not been proved as a precision measurement. Further work is needed to establish the absolute reliability of the measurements. Until the precision is established and confirmed by a tradition of experience, such as that behind the measurement of major neutral and ion densities, uncertainties in the theory cannot be reduced further. ENGEBRETSON *et al.* (1977b) have derived an empirical model for the N density at 375 km which reproduces the seasonal diurnal and latitudinal variations observed by the OSS instrument. These variations are large.

The importance of atomic nitrogen in the chemistry of the ionosphere was described briefly in Section 3.4.1. In the following two sections we discuss the photochemistry of the metastable constituents O(^1S) and O(^1D) where the presence of atomic nitrogen was found to account for the several aspects of the behavior of these species.

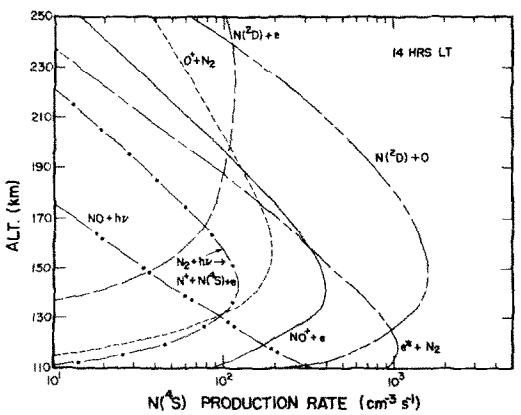

Fig. 32. Daytime sources of N(^4S) derived from AE measurements (RUSCH *et al.*, 1977b).

4.3 *Metastable* O(^{1}D) *atoms*

Sources and sinks of O(^1D) have been studied in detail by HAYS *et al.* (1978) using AE data. Interest

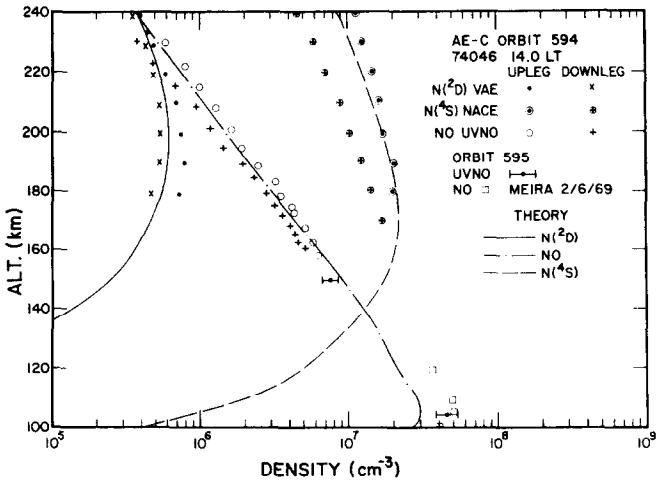

Fig. 33. Measured and theoretical concentrations of odd nitrogen as a function of altitude on AE-C orbit 594. The $N(^2D)$ densities were measured by VAE (HAYS *et al.*, 1973), the $N(^4S)$ by NACE (CARIGNAN and RUSCH, 1978), the NO by the UVNO instrument (BARTH *et al.*, 1973). (cf. CARIGNAN and RUSCH, 1978).

in the photochemistry of $O(^1D)$ has increased recently because of its importance in the stratosphere (CADLE, 1964) and in stratospheric odd nitrogen chemistry (NICOLET, 1971; CRUTZEN, 1970), and because of interest in the ultraviolet neutral heating efficiency and the thermospheric energy budget (CHANDRA and SINKA, 1973; STOLARSKI *et al.*, 1975).

4.3.1 *Sources of thermospheric* $O(^1D)$. Ground state $O(^3P)$ may be excited to the ^1D state in collisions with electrons with energies greater than 1.96 eV.

$$e(E>1.96)+O(^3P)\rightarrow O(^1D)+e. \quad (4.13)$$

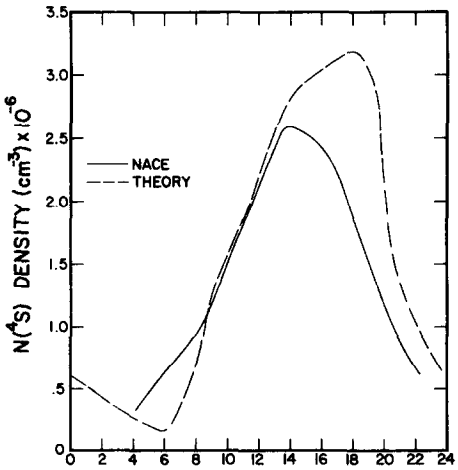

Fig. 34. The diurnal variations of $N(^4S)$ at ~245 km altitude (CARIGNAN and RUSCH, 1978).

The classical nighttime source is dissociative recombination of O_2^+ (BATES, 1946):

$$O_2^+ + e \xrightarrow{\beta_5\alpha_2} O(^1D)+O. \quad (4.14)$$

Photodissociation of O_2:

$$O_2(X^3\Sigma_g^-)+h\nu \xrightarrow{J_{02}} O(^1D)+O(^3P). \quad (4.15)$$

4.3.2 *Sinks of* $O(^1D)$. The main sinks are:

$$O(^1D) \longrightarrow O(^3P)+h\nu, \quad (4.16)$$

$$O(^1D)+N_2 \xrightarrow{k_{30}} O(^3P)+N_2, \quad (4.17)$$

$$O(^1D)+O_2 \xrightarrow{k_{31}} O(^3P)+O_2. \quad (4.18)$$

With the exception of dissociation in the Schumann–Runge continuum of O_2 where the cross section is well-known, there were many uncertainties in the cross sections and rates at which the above processes occur prior to AE.

Excitation cross sections for (4.13) had been derived by HENRY *et al.* (1969). REES (1967) had evaluated the excitation rate by hot thermal electrons and presented a simple expression for the ionization rate as a function of T_e. FOURNIER and NAGY (1965) determined the source due to photoelectrons and hot thermal secondary electrons. However, significant discrepancies arose in the case of the photoelectron flux spectrum. Although the cross sections for photodissociation of O_2 in the Schumann–Runge continuum are well-known (METZER and COOK, 1964; HUDSON, 1971) the absolute value of the solar flux was not well established ($2\times10^{-6}<J_{O_2}(\infty)<6\times10^{-6}\,s^{-1}$). The rates at which $O(^1D)$ is quenched by O_2 and N_2 were also

uncertain prior to AE, despite the fact that the rate had been extensively investigated (e.g. PETERSON and VANZANDT, 1969; HERNANDEZ, 1972; CLARK and NOXON, 1972; HEIDNER and HUSAIN, 1973; SHARP *et al.*, 1975; RUSCH *et al.*, 1975b). Values derived for k_{30} ranged from 2.2×10^{-11} to 1×10^{-10} cm^3 s^{-1}. The rate of O_2 quenching is of the same order as N_2, but the O_2 concentration is much smaller.

HAYS *et al.* (1978) effectively eliminated all the uncertainties discussed above in a comprehensive study of the 6300 Å emission arising from the transition $O(^1S-^1D)$. These measurements were made by the visible airglow experiment described by HAYS *et al.* (1973).

4.3.3 *Nighttime results.* HAYS *et al.* (1978) determined the yield of $O(^1D)$ atoms due to dissociative recombination of O_2^+ at night (4.14) when the latter process constitutes the only significant source. Under these conditions the volume emission rate is given as

$$\eta_{6300}=\frac{A_{6300}\beta_5\alpha_2[O_2^+][N_e]}{A_{^1D}+k_{30}[N_2]}, \qquad (4.19)$$

where A_{6300} is the Einstein coefficient for the transition $O(^1S-^1D)$ and $A_{^1D}$ is the inverse radiative lifetime. Equation (4.19) was rearranged to obtain a linear expression for which β_5 was determined from the intercept and k_{30} from the slope. These results yielded the values

$$\beta_5=1.3, \qquad (4.20)$$

$$k_{30}=3\times10^{-11}\ \text{cm}^3\ \text{s}^{-1}. \qquad (4.21)$$

The latter result is in agreement with earlier rocket determinations of k_{30} (RUSCH *et al.*, 1975b; SHARP *et al.*, 1975). Most ground based determinations of k_{30} however, have yielded values about a factor of two or more larger than this. M. TORR *et al.* (1975) identified the discrepancy as being due to effect of reactions of atomic nitrogen on the concentration of O_2^+, i.e. reaction (3.9). The N density is frequently large enough below 220 km to become a significant loss process for O_2^+. In determining k_{30} from ground based measurements of 6300 Å emission, the O_2^+ density must be calculated. This has been done neglecting (3.9) and the density is overestimated resulting in an overestimation of k_{30} or an under estimation of β_5. In the case of the rocket and satellite experiments, the O_2^+ concentration was measured directly.

4.3.4 *Daytime results.* During the daytime the main sources of $O(^1D)$ are due to (4.13) (photoelectrons) and (4.15) (photodissociation of O_2). HAYS *et al.* (1978) point out that despite considerable disagreement on the absolute magnitude of the photoelectron flux spectrum there has been reasonably good agreement on the shape of the theoretical source due to (4.15). They therefore evaluated the rate of $O(^1D)$ production by photoelectrons. This was found to agree with the theoretical results of DALGARNO and LEJEUNE (1971).

A comparison of the altitude profiles of the sources due to (4.13) and (4.15) shows that the photodissociation source predominates at lower altitudes, and could be studied independently of that due to photoelectrons. Figure 35 shows the $O(^1D)$

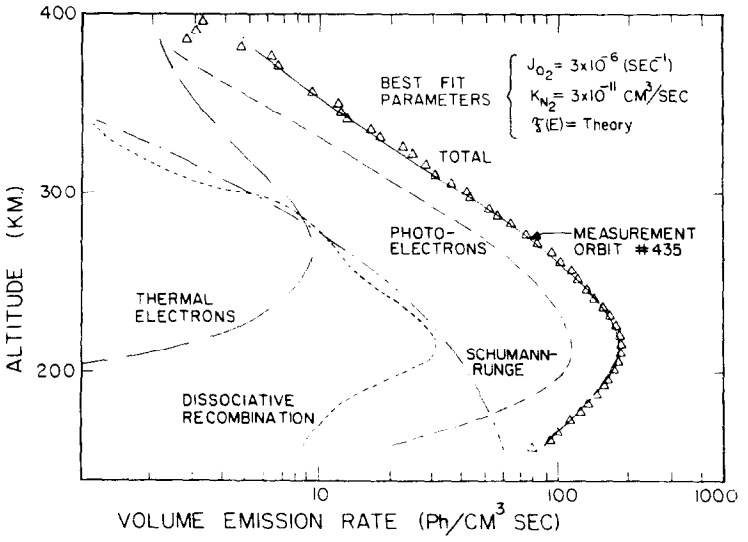

Fig. 35. The volume emission rate of O I (6300 Å) dayglow obtained on AE-C orbit 435 and the theoretical results of HAYS *et al.* (1978).

sources on orbit 435 determined by HAYS *et al.* (1978). They found that $J_{02}(\infty) = 2 \times 10^{-6}\ s^{-1}$. Recent measurements including those done on AE support the lower value for $J_{02}(\infty)$. However, the derivation discussed above involved a factor ~2 uncertainty in the O_2 density.

Figure 36 shows the diurnal variations of the 6300 Å volume emission at 170 km altitude observed and calculated by HAYS *et al.* (1978). The agreement between experiment and theory is good.

4.3.5 *Summary.*

(1) The conventional theory of the 6300 Å dayglow including direct electron excitation of $O(^3P)$, photodissociation of O_2 and dissociative recombination of O_2^+ explains the measured 6300 Å dayglow.

(2) The quenching rate of $O(^1D)$ by N_2 is about a factor of 2 lower than that deduced from ground based measurements. This is due to neglect of destruction of O_2^+ by N in ground based studies. The rate coefficient was found to be $3 \pm 1 \times 10^{-11}\ cm^3\ s^{-1}$.

(3) The efficiency for the production of $O(^1D)$ atoms by dissociative recombination of O_2^+ is 1.3 ± 0.3.

4.4 *Metastable* (^1S) *atoms*

Investigations prior to AE established the following possible sources of $O(^1S)$ in the thermosphere

$$e + O \longrightarrow O(^1S) + e, \tag{4.22}$$

$$O_2^+ + e \xrightarrow{\beta_6\alpha_2} O(^1S) + O. \tag{4.23}$$

Investigations by WALLACE and MCELROY (1966), FELDMAN *et al.* (1971) SCHAEFER *et al.* (1972) and HAYS and SHARP (1973) established processes (4.22) and (4.23) as significant sources of $O(^1S)$ atoms above 140 km, but considerable conflict existed as to their relative importance. Laboratory measurements by MEYER *et al.* (1969,

Table 4. Thermospheric rate coefficients

Reaction	Rate coefficient ($cm^3\ s^{-1}$)	
$NO^+ + e \xrightarrow{\beta_1\alpha_1} N(^2D) + O$	$\beta_1 \approx 1.0$	FREDERICK and RUSCH (1977)
$N_2^+ + e \xrightarrow{\alpha_{82\to3}} N(^2D) + N$	$\beta_1 \approx 1.0$	FREDERICK and RUSCH (1977)
$N_2^+ + O \xrightarrow{\beta_1 k_9} N(^2D) + NO^+$	$\beta_1 \approx 1.0$	FREDERICK and RUSCH (1977)
$N^+ + O_2 \xrightarrow{k_{24}} N(^2D) + O_2^+$	4×10^{-10}	HUNTRESS and ANICICH (1976)
$N(^2D) + O \xrightarrow{k_{25}} N(^4S) + O$	$4 \pm 2 \times 10^{-13}$	FREDERICK and RUSCH (1977)
$N(^2D) + O_2 \xrightarrow{k_{25}} NO + O$	$6 \pm 1 \times 10^{-12}$	FREDERICK and RUSCH (1977)
$N(^2D) + e \xrightarrow{k_{26}} N(^4S) + e$	$3.6 - 6.5 \times 10^{-10}\ (T_e/300)^{1/2}$	FREDERICK and RUSCH (1977)
$N(^2D) + O \xrightarrow{k_{28}} NO^+ + e - 0.37\ eV$	$< 2 \times 10^{-13}$	M. TORR and TORR (1979b)
$N(^4S) + O_2 \xrightarrow{k_{27}} NO^+ + O$	$2.4 \times 10^{-11}\ e^{-3975/T}$	WILSON (1967)
$N(^4S) + NO \xrightarrow{k_{28}} N_2 + O$	$1.5 \times 10^{-12}\ T^{1/2}$	PHILLIPS and SCHIFF (1962)
$O_2^+ + e \xrightarrow{\beta_5\alpha_2} O(^1D) + O$	$\beta = 1.3 \pm 0.3$	HAYS *et al.* (1978)
$O_2(X^3\Sigma_g^-) + h\nu \xrightarrow{J_{O_2}} O(^1D) + O(^3P)$	$J_{O_2} = 2 \times 10^{-6}\ s^{-1} \pm 50\%$	HAYS *et al.* (1978)
$O(^1D) + N_2 \xrightarrow{k_{30}} O(^3P) + N_2$	$3 \pm 1 \times 10^{-11}$	HAYS *et al.* (1978)
$O_2^+ + e \xrightarrow{\beta_6\alpha_2} O(^1S) + O$	$\beta_6 \approx 0.8$	FREDERICK *et al.* (1976)
$O_2^+ + N \xrightarrow{k_{33}} NO^+ + O(^1S)$	$\beta_6\alpha_2 = 7.4 \pm 0.8 \times 10^{-9}(T_e/1150)^{-0.17} \approx 2.5 \times 10^{-11}$	FREDERICK *et al.* (1976)

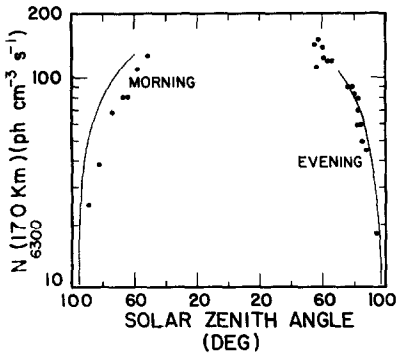

Fig. 36. Plot of the theoretical and experimental 6300 Å volume emission rates at 170 km vs solar zenith angle for morning and evening twilight. The circles are the VAE data; the solid lines are the model results of HAYS *et al.* (1978).

1970) indicated that the charge transfer reaction

$$N_2(A^3\Sigma^+) + O \xrightarrow{k_{32}} N_2 + O(^3P, {}^1D, {}^1S), \quad (4.24)$$

yields a significant fraction of $O(^1S)$ atoms. Radiative loss at 5577 Å constitutes the only significant sink for $O(^1S)$ above 140 km. The radiative lifetime is 0.75 s (GARSTUNG, 1956).

FREDERICK *et al.* (1976) analyzed the AE VAE measurements of the 5577 Å green line which arises from the transition $O(^1D-{}^1S)$. Their approach was similar to that of HAYS *et al.* (1978) for $O(^1D)$. They used nighttime measurements to determine β_6, i.e. when the photoelectron source of $O(^1S)$ (4.22) is negligible. They found that $\beta_6 \simeq 0.8$. Figure 37 shows a comparison of the theoretical and measured 5577 Å volume emission rates on one orbit at night.

Analysis of the daytime VAE measurements clearly indicated that nearly all of the observed emission above 200 km could be accounted for by reactions (4.22) and (4.23) (FREDERICK *et al.*, 1976). Results for AE-C orbit 2744 are shown in Fig. 38. It was evident that a significant additional source is required below 200 km. FREDERICK *et al.* (1976) identified this as the reaction

$$O_2^+ + N \xrightarrow{k_{33}} NO^+ + O(^1S) \quad (4.25)$$

from the scale height characteristics required. The source due to (4.24) ($N_2 - A + O$) was rejected because it was not large enough. The upper limit that FREDERICK *et al.* used arose mainly from an efficiency of 10% adopted for the $O(^1S)$ yield. This was based on auroral rocket measurements. An analysis of the diurnal variation of the green line emission by KOPP *et al.* (1977a) provided convincing evidence that (4.25) accounted for the broad features of the observed temporal variations in $[O(^1S)]$ adequately. The $O(^1S)$ emission exhibits a slow rise in the morning which builds up during the day and then decreases gradually as sunset approaches. This variation is not consistent with the temporal behavior of N_2A which is excited primarily by photoelectron impact. Atomic nitrogen, however, exhibits just the right kind of diurnal variation required to account for the observed green line emission. Unfortunately, measurements of [N] were not available over a diurnal cycle and hence the comparison was not strictly quantitative.

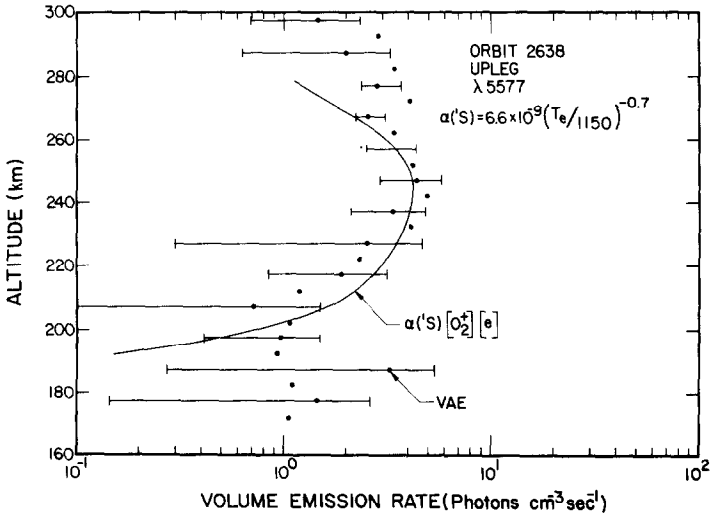

Fig. 37. 5577 Å volume emission rate for nighttime orbit 2638 upleg (3 August 1974). The solid line is a theoretical fit to the VAE data using O_2^+ measured by BIMS and electron densities from the CEP experiment (FREDERICK *et al.*, 1976).

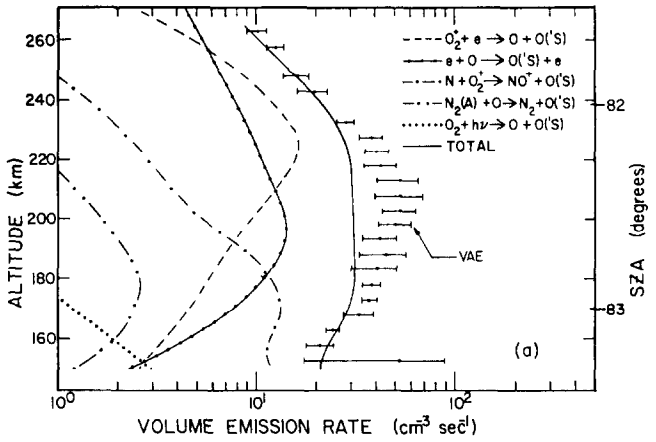

Fig. 38. The twilight 5577 Å volume emission rate for the downleg of AE-C orbit 2744, 11 August 1974 (FREDERICK *et al.*, 1976).

KOPP *et al.* (1977a) deduced that $k_{33} = 2.5 \times 10^{-11}$ cm s^{-1} and

$$\beta_6\alpha_2 = 7.4 \pm 0.8 \times 10^{-9}(T_e/1150)^{-0.7}.$$

It should be noted that the temperature dependence is an assumed laboratory value which applies to cases for $T_e \leq 1200$ K. FREDERICK *et al.* (1976) found the temperature dependence above 1200 K to agree with the laboratory measurements of MEHR and BIONDI (1969). They also investigated several other possible sources of $O(^1S)$ which were all rejected as insignificant.

4.4.1 *Summary.* There are three main sources of $O(^1S)$ in the thermosphere above 150 km. These are photoelectron impact on O, dissociative recombination of O_2^+ and the reaction of atomic nitrogen with O_2^+.

4.5 *The second positive system of* N_2

The $N_2(2P)(0\text{–}0)$ transition at 3371 Å was measured by VAE. The primary reason for monitoring this emission, which is excited by electron impact was to provide a monitor of the photoelectron flux. In view of the controversy that has arisen over the absolute values of the fluxes measured by the photoelectron spectrometer of DOERING *et al.* (1973), the 3371 Å measurement has provided valuable additional information to modelers.

The dayglow emission was first identified by BARTH and PEARCE (1966). The volume emission rate was first calculated by NAGY and FOURNIER (1965). The relationship between the measured 3371 Å volume emission rate and that calculated using measured photoelectron flux cross section data was established by DOERING *et al.* (1970).

Figure 39 shows the measured volume emission rates observed on AE-D orbit 1788 (D) with the theoretical calculations of KOPP *et al.* (1977b). The theoretical values were derived using two model calculations of the photoelectron flux spectrum. The 'Roble model' is essentially the same as that used by NAGY *et al.* (1977).

KOPP *et al.* (1977b) observed a sharp dependence of the emission on the $[O]/[N_2]$ ratio. This was attributed to competition by O in the attenuation of the primary photoelectrons. Also atomic oxgyen and molecular nitrogen have different photoionization cross sections and produce different primary photoelectron energy distributions for a given strong solar line. Although this does average out to

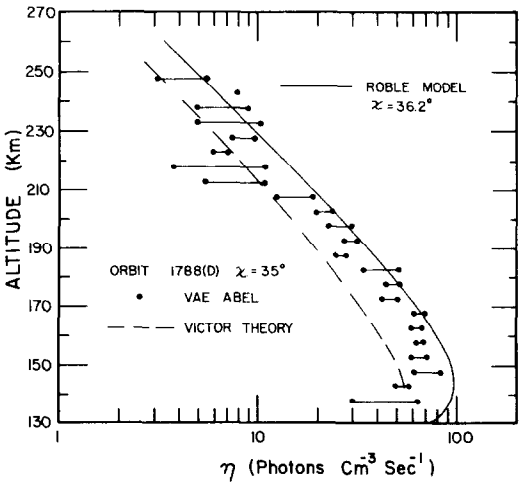

Fig. 39. Comparison of VAE 3371 Å $N_2(^2P)$ (O——O) data (solid circles) with calculations (broken line, G. VICTOR; solid line, R. ROBLE) (KOPP *et al.*, 1977b).

some extent, if the $N_2(2P)$ dayglow emissions are used to monitor the photoelectron flux, these effects must be taken into consideration.

5. DISCUSSION AND CONCLUSION

We have reviewed highlights of the Atmosphere Explorer program involving studies of the chemistry of the ionosphere and thermosphere. Results from the program have exceeded the design goals. Significant results reviewed include the following.

The extreme ultraviolet spectrophotometers have revealed unexpected variations in the EUV flux and in the response of the thermosphere. A long-standing uncertainty concerning the absolute magnitude of the EUV flux has been resolved, and tables of EUV absorption and ionization cross sections and fluxes are presented. Complete references are cited in the text.

The discrepancy between measured and the calculated photoelectron flux is reviewed. No universally acceptable answer to this problem has yet been found. Comparison of theoretical and measured values of several atmospheric emissions excited by electron impact strongly suggest that the measurements are high. The question of the importance of photoelectrons as a source of $O^+(2D)$ and $O^+(2P)$ ions is reviewed. The conclusion is drawn that an upper limit for the photoelectron source is about 15% of the EUV source for $O^+(2P)$.

Recent developments in the detection of nocturnal mid- and low-latitude sources of ionization are briefly reviewed. Ground based results by TINSLEY (1978) point to the existence of an equatorial aurora which could involve an energy deposition rate as large as the polar aurora during magnetic storms. The energy is distributed over a much larger area, however, and the fluxes are low.

The AE data have been used to study many ionospheric and thermospheric processes and numerous rate coefficients have been determined. Major developments in this area are reviewed in some detail, and the most recent results available have been presented. Discrepancies with laboratory results are investigated and reasons for these discrepancies sought.

The photochemical results of the AE program demonstrate that with the data base provided by the three spacecraft it has become possible to use the atmosphere as a laboratory to study atomic and molecular processes.

Only a limited number of studies have been covered in this review. For example, we have omitted results on minor ions and neutrals, such as H, H_e, H^+, H_e^+, O^{2+}. Work on N_2^+, H and M_g emissions have been omitted. Very little space is devoted to variations in the major neutral constituents including the neutral temperature. No discussion is devoted to the energy balance of the thermosphere, and this list is not complete. The results that we present serve to illustrate the broad areas of progress that have been achieved with the AE system. We believe that excellent opportunities exist in space science for rigorously testing theoretical predictions pertaining to many areas of the Physical and Natural sciences.

Acknowledgements—The data used in the studies reviewed in this paper were provided by the AE team. Their collaborative efforts are gratefully acknowledged. This work was supported by NASA grant NAS5-24331, NSF grant ATM75-03986A01 and AF grant F19628-77-C-0007. We thank Dr J. C. G. WALKER for reading the manuscript.

REFERENCES

ALBRITTON D. L., DOTAN I., LINDINGER W., MCFARLAND M., TELLINGHUISEN J. and FEHSENFELD F. C. 1977 *J. chem. Phys.* **66,** 410.

BANKS P. M., SCHUNK R. W. and RAITT W. J. 1974 *Geophys. Res. Lett.* **1,** 239.

BARDSLEY J. N. 1968 *J. Phys. B.* **1,** 365.

BARTH C. A. and PEARCE J. B. 1966 *Space Res.* **6,** 381.

BARTH C. A., RUSCH D. W. and STEWART A. I. 1973 *Radio Sci.* **8,** 379.

BATES D. R. 1946 *Mon. Not. R. astr. Soc.* **106,** 509.

BENSON R. F., BAUER P., BRACE L. H., CARLSON H. C., HAGEN J., HANSON W. B., HOEGY W. R., TORR M. R., WAND R. H. and WICKWAR V. B. 1977 *J. geophys. Res.* **82,** 23.

BLACK G., SLANGER T. C., ST JOHN G. A. and YOUNG R. A. 1969 *J. chem. Phys.* **51,** 116.

BRACE L. H., THEIS R. F. and DALGARNO A. 1973 *Radio Sci.* **8,** 341.

BREIG E. L., TORR M. R., TORR D. G., HANSON W. B., HOFFMAN J. H., WALKER J. C. G. and NIER A. O. 1977 *J. geophys. Res.* **82,** 1008.

BRINTON H. C., SCOTT L. R., PHARO III M. W. and COULSON J. T. C.	1973	*Radio Sci.* **8,** 323.
BRINTON H. C., GREBOWSKY J. M. and BRACE L. H.	1978	*J. geophys. Res.* **83,** 4767.
BURNSIDE R., TORR D. G., MERIWETHER J. W. and TORR M. R.	1978	Paper presented at the Spring Meeting of the *Am. geophys. Un.*, Miami, Florida.
CADLE R. D.	1964	*Discuss. Faraday Soc.* **37,** 66.
CARIGNAN G. R. and RUSCH D. W.	1978	Abstract in *EOS* **59,** 339.
CHANDRA S. and SINKA A. K.	1973	*Planet. Space Sci.* **21,** 593.
CLARK I. D. and NOXON J. F.	1972	*J. chem. Phys.* **57,** 1033.
CRUTZEN P. J.	1970	*Q. Jl R. met. Soc.* **96,** 320.
DALGARNO A. and LEJEUNE G.	1971	*Planet. Space Sci.* **19,** 1653.
DALGARNO A., HANSON W. B., SPENCER N. W. and SCHMERLING E. R.	1973	*Radio Sci.* **8,** 263.
DAVENPORT J. E., SLANGER T. G. and BLACK G.	1976	*J. geophys. Res.* **81,** 12.
DOERING J. P., FASTIE W. G. and FELDMAN P. D.	1970	*J. geophys. Res.* **75,** 4787.
DOERING J. P., BOSTROM C. O. and ARMSTRONG J. C.	1973	*Radio Sci.* **8,** 387.
DONAHUE T. M.	1968	*Science, N.Y.* **159,** 489.
DONAHUE T. M., ZIPF E. C. and PARKINSON T. D.	1970	*Planet. Space Sci.* **18,** 171.
ENGEBRETSON M. J., MAUERSBERGER K. and POTTER W. E.	1977a	*J. geophys. Res.* **82,** 3291.
ENGEBRETSON M. J., MAUERSBERGER K., KAYSER D. C. and NIER A. O.	1977b	*J. geophys. Res.* **82,** 461.
FELDMAN P. D. and TAKACS P. Z.	1974	*Geophys. Res. Lett.* **1,** 169.
FELDMAN P. D., DOERING J. P. and ZIPF E. C.	1971	*J. geophys. Res.* **76,** 3087.
FOURNIER J. P. and NAGY A. F.	1965	*J. atmos. Sci.* **22,** 732.
FREDERICK J. E. and RUSCH D. W.	1977	*J. geophys. Res.* **82,** 3509.
FREDERICK J. E., RUSCH D. W., VICTOR G. A. SHARP W. E., HAYS P. B. and BRINTON H. C.	1976	*J. geophys. Res.* **81,** 3923.
GARSTANG R. H.	1956	*The Airglow and the Aurora.* Pergamon Press, London.
GERARD J. C.	1975	*Geophys. Res. Lett.* **2,** 179.
GHOSH S. N., HINTON B. B., JONES L. M., LEITE R. J., MASON C. J., SCHAEFER E. J. and WALTERS M.	1968	*J. geophys. Res.* **73,** 4425.
GOLDAN P. D., SCHMELTEKOPF A. F., FEHSENFELD F. C., SCHIFF I. and FERGUSON E. E.	1966	*J. chem. Phys.* **44,** 4103.
HANSON W. B., ZUCCARO D. R., LIPPINCOTT C. R. and SANATANI S.	1973	*Radio Sci.* **8,** 333.
HAYS P. B. and SHARP W. E.	1973	*J. geophys. Res.* **78,** 1153.
HAYS P. B., CARIGNAN G. R., KENNEDY B. C., SHEPHERD G. C. and WALKER J. C. G.	1973	*Radio Sci.* **8,** 369.
HAYS P. B., RUSCH D. W., TORR D. G., SHARP W. E. and SWENSON G. R.	1975	*EOS* **56,** 405.
HAYS P. B., RUSCH D. W., ROBLE R. G. WALKER J. C. G.	1978	*Rev. Geophys. Space Phys.* **16,** 225.
HEDIN A. E., MAYR H. G., REBER C. A., SPENCER N. W. and CARIGNAN G. R.	1974	*J. geophys. Res.* **79,** 215.
HEDIN A. E., SPENCER N. W., HANSON W. B. and BAUER P.	1976	*Geophys. Res. Lett.* **3,** 469.
HEDIN A. E., SALAH J. E., EVANS J. V., REBER C. A., NEWTON G. P., SPENCER N. W., KAYSER D. C., ALCAYDE D., BAUER P., COGGER L. and MCCLURE J. P.	1977a	*J. geophys. Res.* **82,** 2139.
HEDIN A. E., REBER C. A., NEWTON G. P., SPENCER N. W., BRINTON H. C., MAYR H. G. and POTTER W. E.	1977b	*J. geophys. Res.* **82,** 2148.
HEIDNER R. F. and HUSAIN D.	1973	*Nature, Lond.* **241,** 10.
HENRY R. J. W.	1970	*Astrophys. J.* **161,** 1153.
HENRY R. J. W. and WILLIAMS R. E.	1968	*Publs. astr. Soc. Pacif.* **80,** 669.
HENRY R. J. W., BURKE P. G. and SINFAILAM A. L.	1969	*Phys. Rev.* **178,** 218.
HERNANDEZ G.	1972	*J. geophys. Res.* **77,** 3625.
HERNANDEZ G. and TURTLE J. P.	1969	*Planet. Space Sci.* **17,** 675.
HINTEREGGER H. E.	1976	*J. atmos. terr. Phys.* **38,** 791.
HINTEREGGER H. E., BEDO D. E. and MANSON J. E.	1973	*Radio Sci.* **8,** 349.

Hinteregger H. E., Bedo D. E., Manson J. E. and Skillman D. R.	1977	*Space Res.* **17,** 533.
Hoegy W. R. and Brace L. H.	1978	*Geophys. Res. Lett.* **5,** 269.
Hoffman J. H., Hanson W. B., Lippincott C. R. and Ferguson E. E.	1973	*Radio Sci.* **8,** 315.
Hoffman R. A., Burch J. L., Janetzke R. W., McChesney J. F., Way S. H. and Evans D. S.	1973	*Radio Sci.* **8,** 393.
Huang C. M., Biondi M. A. and Johnsen R.	1975	*Phys. Rev.* **A11,** 901.
Hudson R. D.	1971	*Rev. Geophys. Space Phys.* **9,** 305.
Huntress W. T. and Anicich V. G.	1976	*Geophys. Res. Lett.* **3,** 317.
Jasperse J. R.	1978	*EOS* **59,** 333.
Keneshea T. J., Narcisi R. S. and Swider W.	1970	*J. geophys. Res.* **75,** 845.
Kirby-Docken K. and Oppenheimer M.	1977	*J. geophys. Res.* **82,** 3503.
Kopp J. P., Frederick J. E., Rusch D. W. and Victor G. A.	1977a	*J. geophys. Res.* **82,** 4715.
Kopp J. P., Rusch D. W., Roble R. G., Victor G. A. and Hays P. B.	1977b	*J. geophys. Res.* **82,** 555.
Lin C. L. and Kaufman F.	1971	*J. chem. Phys.* **55,** 3760.
Lindinger W., Fehsenfeld F. C., Schmeltekopf A. L. and Ferguson E. E.	1974	*J. geophys. Res.* **79,** 4753.
Lindinger W., Albritton D. L., Fehsenfeld F. C. and Ferguson E. E.	1975	*J. geophys. Res.* **80,** 3725.
Mauersberger K., Engebretson M., Potter W. E., Kayser D. C. and Nier A. O.	1975	*Geophys. Res. Lett.* **2,** 337.
McFarland M., Albritton D. L., Fehsenfeld F. C., Ferguson E. E. and Schmeltekopf A. L.	1973	*J. chem. Phys.* **59,** 6620.
McFarland M., Albritton D. L., Fehsenfeld F. C., Ferguson E. E. and Schmeltekopf A. L.	1974	*J. geophys. Res.* **79,** 2925.
Mehr F. J. and Biondi M. A.	1969	*Phys. Rev.* **181,** 264.
Meriwether J. W. and Walker J. C. G.	1977	*J. geophys. Res.* **82,** 1855.
Meriwether J. W. and Walker J. C. G.	1978	*J. atmos. terr. Phys.* **83,** 3311.
Meriwether J. W., Torr D. G. and Walker J. C. G.	1978	*J. geophys. Res* (in press).
Metzer P. A. and Cook G. R.	1964	*J. quantum Spectrosc. Radiat. Transfer* **4,** 107.
Meyer J. A., Setser D. W. and Stedman D. H.	1969	*Astrophys. J.* **157,** 1023.
Meyer J. A., Setser D. W. and Stedman D. H.	1970	*J. phys. Chem., Ithaca* **74,** 2238.
Nagy A. F. and Fournier J. P.	1965	*J. geophys. Res.* **70,** 5981.
Nagy A. F., Doering J. P., Peterson W. K., Torr M. R. and Banks P. M.	1977	*J. geophys. Res.* **82,** 5099.
Nicolet M.	1971	*Mesosphere Models and Related Experiments.* D. Reidel, Hingham, Massachusetts.
Nier A. O., Potter W. E., Hickman D. R. and Mauersberger K. M.	1973	*Radio Sci.* **8,** 271.
Nier A. O., Potter W. E., Kayser D. C. and Finstad R. G.	1974	*Geophys. Res. Lett.* **1,** 197.
Norton R. B. and Barth C. A.	1970	*J. geophys. Res.* **75,** 3903.
Oppenheimer M., Dalgarno A. and Brinton H. C.	1976	*J. geophys. Res.* **81,** 4678.
Oppenheimer M., Constantinides E. R., Kirby-Docken K., Brinton H. C. and Hoffman J. H.	1977a	*J. geophys. Res.* **82,** 5485.
Oppenheimer M., Dalgarno A., Trebino F. P., Brace L. H., Brinton H. C. and Hoffman J. H.	1977b	*J. geophys. Res.* **82,** 191.
Oppenheimer M., Babeu S., Hoffman J. H. and Breig E.	1978	*Geophys. Res. Lett.* **5,** 773.
Oran E. S., Julienne P. S. and Strobel D. F.	1975	*J. geophys. Res.* **80,** 3068.
Orsini N., Torr D. G., Torr M. R., Brinton H. C., Brace L. H., Nier A. O. and Walker J. C. G.	1977a	*J. geophys. Res.* **82,** 4829.
Orsini N., Torr D. G., Brinton H. C., Brace L. H., Hanson W. B., Hoffman J. H. and Nier A. O.	1977b	*Geophys. Res. Lett.* **4,** 431.

PAULIKAS G. A.	1975	*Rev. Geophys. Space Phys.* **13,** 709.
PELZ D. R., REBER C. A., HEDIN A. E. and CARIGNAN G. R.	1973	*Radio Sci.* **8,** 277.
PETERSEN W. L., DOERING J. P., POTEMSA T. A. and BOSTROM C. O.	1977	JHA/APL Preprint 77-05, NATO *Advd Study Insts Ser.*, D. Reidel.
PETERSON V. L. and VANZANDT T. E.	1969	*Planet. Space Sci.* **17,** 1725.
PHILLIPS J. F. and SCHIFF H. I.	1962	*J. chem. Phys.* **36,** 1509.
PRATHER M. J., MCELROY M. B. and RODRIGUES J.	1978	*Planet. Space Sci.* **26,** 131.
PRÖLSS G. W.	1975	*Annls geophys.* **29,** 503.
REES M. H.	1967	*Planet. Space Sci.* **15,** 1097.
ROBLE R. G.	1975	*Planet. Space Sci.* **23,** 1017.
RUSCH D. W.	1973	*J. geophys. Res.* **78,** 5676.
RUSCH D. W., STEWART A. I., HAYS P. B. and HOFFMAN J. H.	1975a	*J. geophys. Res.* **80,** 2330.
RUSCH D. W., SHARP W. E. and HAYS P. B.	1975b	*J. geophys. Res.* **80,** 1832.
RUSCH D. W., TORR D. G., HAYS P. B. and TORR M. R.	1976	*Geophys. Res. Lett.* **3,** 537.
RUSCH D. W., TORR D. G., HAYS P. B. and WALKER J. C. G.	1977a	*J. geophys. Res.* **82,** 719.
RUSCH D. W., CRAVENS T. E., CARIGNAN G. R., STEWART A. I. and GERARD J.-C.	1977b	*EOS* **58,** 1198.
RUTHERFORD J. A. and VROOM D. A.	1971	*J. chem. Phys.* **55,** 5622.
SCHAEFFER R. C., FELDMAN P. D. and ZIPF E. C.	1972	*J. geophys. Res.* **77,** 6828.
SCHUNK R. W. and WALKER J. C. G.	1973	*Planet. Space Sci.* **21,** 1875.
SCHUNK R. W., BANKS P. M. and RAITT W. J.	1976	*J. geophys. Res.* **81,** 3271.
SEATON M. J.	1956	*The Airglow and the Aurorae.* Pergamon Press, New York, p. 289.
SHARP R. D., JOHNSON R. G. and SHELLEY E. E.	1976	*J. geophys. Res.* **81,** 3292.
SHARP W. E.	1978	*J. geophys. Res.* (in press).
SHARP W. E., RUSCH D. W. and HAYS P. B.	1975	*J. geophys. Res.* **80,** 2876.
SLANGER T. G., WOOD B. J. and BLACK G.	1971	*J. geophys. Res.* **76,** 8430.
SPENCER N. W., NIEMANN H. B. and CARIGNAN G. R.	1973	*Radio Sci.* **8,** 284.
SPIRO R. W., HEELIS R. A. and HANSON W. B.	1978	*J. geophys. Res.* **83,** 4255.
STEBBINGS R. F., TURNER B. R. and RUTHERFORD J. A.	1966	*J. geophys. Res.* **71,** 771.
STOLARSKI R. S., HAYS P. B. and ROBLE R. G.	1975	*J. geophys. Res.* **80,** 2266.
ST-MAURICE J. P. and TORR D. G.	1978	*J. geophys. Res.* **83,** 969.
STROBEL D. F., HUNTEN D. M. and MCELROY M. M.	1970	*J. geophys. Res.* **75,** 4307.
STROBEL D. F., YOUNG T. R., MEIER R. R., COFFEY T. P. and ALI A. W.	1974	*J. geophys. Res.* **71,** 3171.
STROBEL D. F., ORAN E. S. and FELDMAN P. D.	1976	*J. geophys. Res.* **81,** 3745.
TINSLEY B. A.	1979	*J. atmos. terr. Phys.* (to appear).
TORR D. G. and ORSINI N.	1977	*Planet. Space Sci.* **25,** 1171.
TORR D. G. and ORSINI N.	1978	*Geophys. Res. Lett.* **5,** 657.
TORR D. G. and TORR M. R.	1978	*Rev. Geophys.* **16,** 327.
TORR D. G., TORR M. R. and LAURIE D. P.	1972	*J. geophys. Res.* **77,** 203.
TORR D. G., RUSCH D. W., TORR M. R. WALKER J. C. G., HOFFMAN J. H., HAYS P. B. and OPPENHEIMER M.	1974	*EOS Trans. Am. geophys. Un.*, **56,** 1159.
TORR D. G., TORR M. R., HOFFMAN R. A. and WALKER J. C. G.	1976a	*Geophys. Res. Lett.* **3,** 305.
TORR D. G., TORR M. R., WALKER J. C. G., BRACE L. H., BRINTON H. C., HANSON W. B., HOFFMAN J. H., NIER A. O. and OPPENHEIMER M.	1976b	*Geophys. Res. Lett.* **3,** 209.
TORR D. G., TORR M. R., WALKER J. C. G., NIER A. O., BRACE L. H. and BRINTON H. C.	1976c	*J. geophys. Res.* **81,** 5578.
TORR D. G., TORR M. R., RUSCH D. W., HAYS P. B., MAUERSBERGER K., WALKER J. C. G., SPENCER N. W., HEDIN A. E., BRINTON H. C. and THEIS R. F.	1976d	*Geophys. Res. Lett.* **3,** 1.
TORR D. G., ORSINI N., TORR M. R., HANSON W. B., HOFFMAN J. H. and WALKER J. C. G.	1977	*J. geophys. Res.* **82,** 1631.

TORR D. G., DONAHUE K., RUSCH D. W., TORR M. R., NIER A. O., KAYER D., HANSON W. B. and HOFFMAN J. H.	1978	*J. geophys. Res.* (in press).
TORR M. R., WALKER J. C. G. and TORR D. G.	1974	*J. geophys. Res.* **79,** 5267.
TORR M. R., TORR D. G., WALKER J. C. G., HAYS P. B., HANSON W. B., HOFFMAN J. H. and KAYSER D. C.	1975	*Geophys. Res. Lett.* **2,** 395.
TORR M. R., HAYS P. B., KENNEDY B. C. WALKER J. C. G.	1977a	*Planet. Space Sci.* **25,** 173.
TORR M. R., ST-MAURICE J. P. and TORR D. G.	1977b	*J. geophys. Res.* **22,** 3287.
VICTOR G. A., KIRBY-DOCKEN K. and DALGARNO A.	1976	*Planet. Space Sci.* **24,** 679.
WALKER J. C. G., TORR D. G., HAYS P. B., RUSCH D. W., KIRBY-DOCKEN K., VICTOR G. and OPPENHEIMER M.	1975	*J. geophys. Res.* **80,** 1026.
WALLACE L. and MCELROY M. B.	1966	*Planet. Space Sci.* **14,** 667.
WALLS F. L. and DUNN G. H.	1974	*J. geophys. Res.* **79,** 1911.
WEILL G. M.	1969	*Atmospheric Emissions.* Van Nostrand Reinhold, New York.
WILSON W. E.	1967	*J. chem. Phys.* **46,** 2017.
ZIPF E. C.	1978	EOS **59,** 336.

Reference is also made to the following unpublished material:

HEROUX L. and HINTEREGGER H. E.	1978	Submitted to *J. geophys. Res.*
HINTEREGGER H. E.	1978a	Submitted to *J. geophys. Res.*
HINTEREGGER H. E.	1978b	Submitted to *Rev. Geophys. Space Phys.*
KIRBY-DOCKEN, K., CONSTANTINEDES R., BABEU S. OPPENHEIMER M. and VICTOR G. A.	1978	Submitted to *Atomic Data.*
MICHELS H. H.	1974	Report AFWL-TR-73-288, Air Force Weapons Laboratory, Kirtland Air Force Base, Unpublished.
ORSINI N.	1977	PhD Thesis, University of Michigan.
SWENSON G. R.	1976	PhD Thesis, University of Michigan.
TAKANAYAGI K.	1964	*JILA Rept. 7,* University of Colorado.
TORR D. G.	1979	*J. geophys. Res.* (in press).
TORR D. G., TORR M. R., BRINTON H. C., BRACE L. H., SPENCER N. W., HEDIN A. E., HANSON W. B., HOFFMAN J. H., NIER A. O. and WALKER J. C. G.	1979	*J. geophys. Res.* (in press).
TORR M. R. and TORR D. G.	1979a	*J. geophys. Res.* (in press).
TORR M. R. and TORR D. G.	1979b	*Planet. Space Sci.* (in press).